

4

DTIC FILE COPY

TECHNICAL REPORT CERC-87-16

# COMBINED REFLECTION AND DIFFRACTION BY A VERTICAL WEDGE

by

H. S. Chen

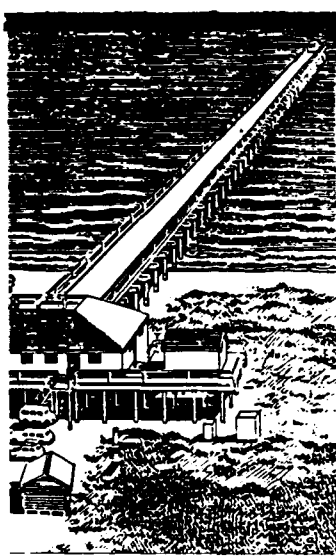
Coastal Engineering Research Center

DEPARTMENT OF THE ARMY  
Waterways Experiment Station, Corps of Engineers  
PO Box 631, Vicksburg, Mississippi 39180-0631

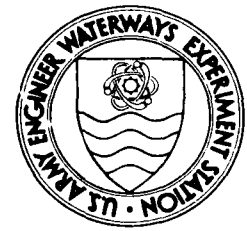
AD-A195 469



US Army Corps  
of Engineers



\*Original contains color  
plates: All DTIC reproductions  
will be in black and  
white.

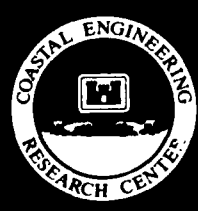
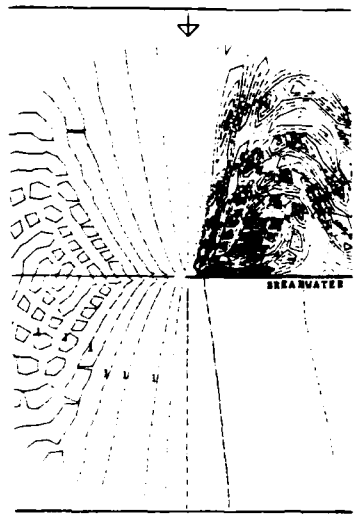


December 1987

Final Report

Approved For Public Release, Distribution Unlimited

DTIC  
ELECTE  
MAY 16 1988  
S D  
E



Prepared for DEPARTMENT OF THE ARMY  
US Army Corps of Engineers  
Washington, DC 20314-1000

Under Waves at Entrances Work Unit 31673

88 5 17 072

Destroy this report when no longer needed. Do not return it  
to the originator.

The findings in this report are not to be construed as an official  
Department of the Army position unless so designated by other  
authorized documents.

This program is furnished by the Government and is accepted and used by  
the recipient with the express understanding that the United States  
Government makes no warranties, expressed or implied, concerning the  
*accuracy, completeness, reliability, usability, or suitability* for any par-  
ticular purpose of the information and data contained in this program or  
furnished in connection therewith, and the United States shall be under no  
liability whatsoever to any person by reason of any use made thereof. The  
program belongs to the Government. Therefore, the recipient further  
agrees not to assert any *proprietary rights therein* or to represent this  
program to anyone as other than a Government program.

The contents of this report are not to be used for  
advertising, *publication, or promotional purposes*.  
Citation of trade names does not constitute an  
official endorsement or approval of the use of such  
commercial products.

Unclassified

SECURITY CLASSIFICATION OF THIS PAGE

112-1495-1000

REPORT DOCUMENTATION PAGE				Form Approved OMB No 0704 0188 Exp Date Jun 30 1986	
1a REPORT SECURITY CLASSIFICATION Unclassified		1b RESTRICTIVE MARKINGS			
2a SECURITY CLASSIFICATION AUTHORITY		3 DISTRIBUTION/AVAILABILITY OF REPORT Approved for public release; distribution unlimited.			
2b DECLASSIFICATION/DOWNGRADING SCHEDULE					
4 PERFORMING ORGANIZATION REPORT NUMBER(S) Technical Report CERC-87-16		5 MONITORING ORGANIZATION REPORT NUMBER(S)			
6a NAME OF PERFORMING ORGANIZATION USAEWES, Coastal Engineering Research Center	6b OFFICE SYMBOL (if applicable)	7a NAME OF MONITORING ORGANIZATION			
6c ADDRESS (City, State, and ZIP Code) PO Box 631 Vicksburg, MS 39180-0631		7b ADDRESS (City, State, and ZIP Code)			
8a NAME OF FUNDING/SPONSORING ORGANIZATION US Army Corps of Engineers	8b OFFICE SYMBOL (if applicable)	9 PROCUREMENT INSTRUMENT IDENTIFICATION NUMBER			
8c ADDRESS (City, State, and ZIP Code) Washington, DC 20314-1000		10. SOURCE OF FUNDING NUMBERS	PROGRAM ELEMENT NO	PROJECT NO	TASK NO
					WORK UNIT ACCESSION NO 31673
11. TITLE (Include Security Classification) Combined Reflection and Diffraction by a Vertical Wedge					
12 PERSONAL AUTHOR(S) Chen, H. S.					
13a TYPE OF REPORT Final report	13b TIME COVERED FROM _____ TO _____	14 DATE OF REPORT (Year, Month, Day) December 1987		15 PAGE COUNT 75	
16. SUPPLEMENTARY NOTATION Available from National Technical Information Service, 5285 Port Royal Road, Springfield, VA 22161.					
17. COSATI CODES		18. SUBJECT TERMS (Continue on reverse if necessary and identify by block number)			
FIELD	GROUP	SUB-GROUP	Breakwaters (LC)		
			Numerical analysis (LC)		
			Water waves (LC)		
19. ABSTRACT (Continue on reverse if necessary and identify by block number) This report presents an analytical solution for the combined wave reflection and diffraction by a vertical wedge, of arbitrary wedge angle, subject to the excitation of a plane simple harmonic wave train coming from a far field. Results of two special cases are calculated: one a thin semi-infinite breakwater and the other a wedge of 90-deg angle. The results are presented in amplification factor diagrams. A subroutine WEDGE is also documented in the appendix. The subroutine can be used to calculate the case of arbitrary wedge angle.					
20 DISTRIBUTION/AVAILABILITY OF ABSTRACT <input checked="" type="checkbox"/> UNCLASSIFIED/UNLIMITED <input type="checkbox"/> SAME AS RPT <input type="checkbox"/> DTIC USERS			21 ABSTRACT SECURITY CLASSIFICATION Unclassified		
22a NAME OF RESPONSIBLE INDIVIDUAL		22b TELEPHONE (Include Area Code)		22c OFFICE SYMBOL	

SECURITY CLASSIFICATION OF THIS PAGE



SECURITY CLASSIFICATION OF THIS PAGE

PREFACE

The work in this report was authorized by the Office, Chief of Engineers (OCE), Coastal Engineering Functional Area of Civil Works Research and Development, under Waves at Entrances Work Unit 31673, Harbor Entrances and Coastal Channels Program, at the Coastal Engineering Research Center (CERC) of the US Army Engineer Waterways Experiment Station (WES). Messrs. John H. Lockhart, Jr., and John G. Housley were OCE Technical Monitors. Dr. Charles L. Vincent is CERC Program Manager.

This report was prepared by Dr. H. S. Chen, Coastal Oceanography Branch (CR-0), Research Division (CR). Work was performed under direct supervision of Dr. Edward F. Thompson, Chief, CR-0, and Mr. H. Lee Butler, Chief, CR; and under general supervision of Dr. James R. Houston and Mr. Charles C. Calhoun, Jr., Chief and Assistant Chief, CERC, respectively.

This study was initiated after a discussion by Dr. Vincent and the author on the possibility of implementing a scheme to redistribute wave energy behind islands in numerical models. The author acknowledges and appreciates the review and comments provided by Drs. Edward F. Thompson and Norman W. Scheffner. This report was edited by Ms. Shirley A. J. Hanshaw, Information Products Division, Information Technology Laboratory, WES.

Commander and Director of WES is COL Dwayne G. Lee, CE, and Technical Director is Dr. Robert W. Whalin.

"Original contains color plates: All DTIC reproductions will be in black and white"



Accession For	
NTIS GRA&I	<input checked="" type="checkbox"/>
DTIC TAB	<input type="checkbox"/>
Unannounced	<input type="checkbox"/>
Justification	
By _____	
Distribution/	
Availability Codes	
Dist	Avail and/or Special
A-1	

CONTENTS

	<u>Page</u>
PREFACE.....	1
PART I: INTRODUCTION.....	3
PART II: BOUNDARY VALUE PROBLEM.....	4
Mathematical Formulation.....	4
Analytical Solution.....	7
Two Special Cases.....	11
PART III: CALCULATION AND RESULTS.....	13
Vertical Wedge of 0-Deg Wedge Angle.....	13
Vertical Wedge of 90-Deg Wedge Angle.....	27
PART IV: CONCLUSION.....	40
REFERENCES.....	41
APPENDIX A: SUBROUTINE WEDGE.....	A1
APPENDIX B: NOTATION.....	B1

## COMBINED REFLECTION AND DIFFRACTION BY A VERTICAL WEDGE

### PART I: INTRODUCTION

1. The boundary value problem of linear wave reflection and diffraction by a vertical wedge of arbitrary wedge angle has been well formulated and presented by Stoker (1957) among many other investigators. The technique to obtain an analytical solution for the problem is also depicted in the cited book. However, analytical solutions are not available for the problem, except for the special case of wave diffraction by a thin semi-infinite breakwater, that is, a wedge with wedge angle equal to zero.

2. The solution of the thin semi-infinite breakwater was presented in the dimensionless diffraction diagrams by Wiegel (1962). The diagrams have been especially useful in preliminary engineering design and have been included in the Shore Protection Manual (SPM) (1984). Although equally useful, the combined reflection and diffraction diagrams are not available, perhaps because of the complexity of the diagrams which makes them difficult to create without using modern high-speed computers for computation and graphing.

3. The objectives of the present study are (a) to obtain an analytical solution for the combined wave reflection and diffraction by a vertical wedge of arbitrary wedge angle subject to excitation of a plane simple harmonic wave train coming from infinity and (b) to provide the combined reflection and diffraction diagrams. The diagrams included in this report have two cases: one for a thin semi-infinite breakwater and the other for a 90-deg vertical wedge. Subroutine WEDGE for computing the combined reflection and diffraction by a vertical wedge of arbitrary wedge angle is also documented in the report (Appendix A).

PART II: BOUNDARY VALUE PROBLEM

Mathematical Formulation

4. In this study our primary interest is the wave reflection and diffraction by a vertical wedge of arbitrary wedge angle in a constant water depth  $h$  \* subject to the excitation of monochromatic incident waves of infinitesimal amplitude coming from infinity. Let  $(r, \theta, z)$  be cylindrical coordinates, with  $z = 0$  representing the undisturbed water free surface and upward direction representing the positive  $z$ -axis. The tip of the wedge is chosen to be the origin of the coordinates and two rigid walls of the wedge to coincide with  $\theta = 0$  and  $\theta = \theta_0$ , respectively, as illustrated in Figure 1. Cartesian coordinates  $(x, y, z)$ , corresponding to the cylindrical coordinates, are also occasionally used and shown in the same figure. Therefore, the wedge

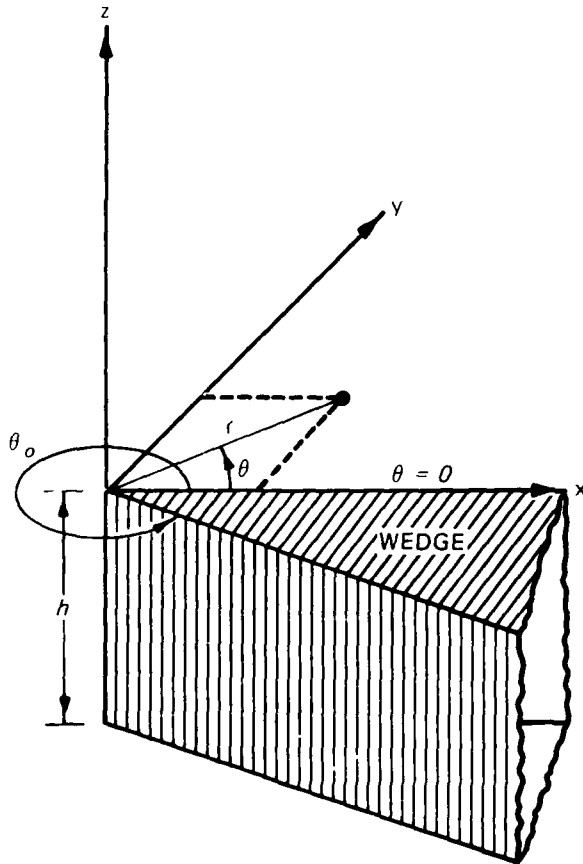


Figure 1. A vertical wedge of arbitrary wedge angle

\* For convenience, symbols and abbreviations are listed in the notation (Appendix B).

angle is  $2\pi - \theta_0$ , and the water region is defined by  $\theta_0 \geq \theta \geq 0$  and  $0 \geq z \geq -h$ .

5. The velocity field for the wave reflection and diffraction in an ideal fluid can be represented by the velocity potential function  $\Phi(r, \theta, z, t)$  which must satisfy the Laplace equation, where  $t$  is the temporal coordinate. We assume that the waves are sinusoidal in time with radian frequency  $\omega$ . Water depth is constant, and the bottom is rigid and impermeable. Therefore, the vertical and temporal components of the velocity potential function, which follow from separation of variables, can be factored out and the velocity potential written as

$$\Phi(r, \theta, z, t) = A_0 \frac{\cosh k(z + h)}{\cosh kh} \phi(r, \theta) e^{i\omega t} \quad (1)$$

where

$$A_0 = -iga_0/\omega$$

$$i = \sqrt{-1}$$

$g$  = gravitational acceleration

$a_0$  = incident wave amplitude

$k$  = wave number

$\phi$  = horizontal component of the velocity potential function

6. Substituting Equation 1 into the Laplace equation and using both the kinematic and dynamic boundary conditions at the free surface, the Laplace equation is then reduced to the Helmholtz equation which is written in polar coordinates as follows:

$$r^2 \frac{\partial^2 \phi}{\partial r^2} + r \frac{\partial \phi}{\partial r} + \frac{\partial^2 \phi}{\partial \theta^2} + k^2 r^2 \phi = 0 \quad (2)$$

where  $k$  must be a real number and satisfy the dispersion relationship

$$\omega^2 = gk \tanh kh \quad (3)$$

7. The free surface displacement  $\eta$  from the mean water level  $z = 0$  can be obtained from linear wave theory and is represented as

$$\eta(r, \theta, t) = \frac{1}{g} \frac{\partial \Phi}{\partial t} = a_0 \phi(r, \theta) e^{i\omega t} \quad (4)$$

8. Thus only the horizontal part of the velocity potential function  $\phi$  is needed to be determined as a solution of Equation 2 in the water region  $\theta_0 \geq \theta \geq 0$ , with the following boundary conditions at the rigid and impermeable walls of the wedge:

$$\frac{\partial \phi}{\partial \theta} = 0 \quad \text{at } \theta = 0 \quad \text{and } \theta_0 \quad (5)$$

9. A condition at infinity is also required to ensure a unique solution. The classic approach is to use the Sommerfeld radiation condition at infinity which states that the scattered wave  $\phi_s$  must behave like a cylindrical outgoing progressing wave at infinity such that

$$\lim_{r \rightarrow \infty} \sqrt{r} \left( \frac{\partial \phi_s}{\partial r} + ik\phi_s \right) = 0 \quad (6)$$

The total wave represented by  $\phi$  is the linear superposition of an incident wave  $\phi_i$ , a reflected wave from the  $\theta = 0$  wall of the wedge  $\phi_r$ , and the scattered wave  $\phi_s$  from the tip of the wedge.

$$\phi = \phi_i + \phi_r + \phi_s \quad (7)$$

Equation 6 can be satisfied if

$$\phi_s \sim \frac{e^{-ikr}}{\sqrt{kr}} \quad \text{at } r \rightarrow \infty \quad (8)$$

10. The incident wave coming from a large distance from the tip of the wedge is assumed to be a plane progressive wave of amplitude  $a_0$  and incident angle  $\alpha$  to the x-axis as given by

$$\phi_i = e^{ikr \cos(\theta - \alpha)} \quad (9)$$

Consequently, the perfectly reflected wave from the  $y = 0$  wall of the wedge is

$$\phi_r = e^{ikr \cos(\theta + \alpha)} \quad (10)$$

Thus the boundary value problem (in which the governing equation is Equation 2, the boundary condition is Equation 5, and the radiation condition is Equation 6) is completely formulated.

### Analytical Solution

11. Analytical solution to the problem formulated in the preceding section is obtained by following the solution technique by Stoker (1957). To obtain the solution, the water region is divided into three subregions--I, II, and III--by the incident wave ray passing through the tip of the wedge and the reflected wave ray reflected away from the tip of the wedge, as shown in Figure 2. Obviously, the total wave in subregion I is the sum of the incident, reflected, and scattered waves; the total wave in subregion II, where the reflected wave does not exist, is the sum of the incident and scattered waves; and the total wave in subregion III, where the incident and reflected waves have been shaded out, is only the scattered wave. For certain combinations of

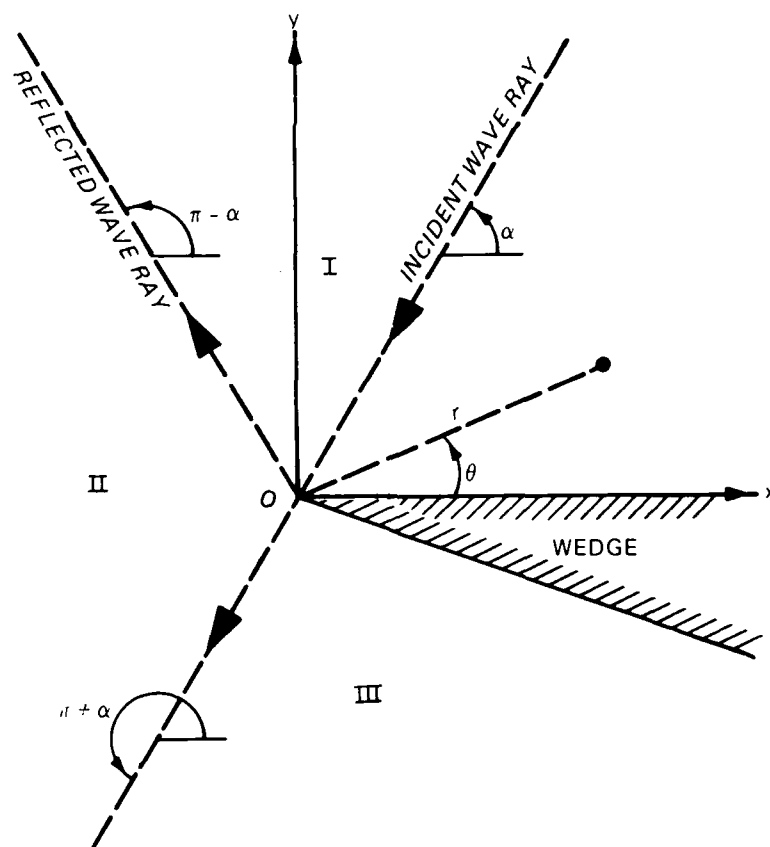


Figure 2. Three subregions and the wedge

the wedge angle and incident wave angle, subregions II and III may not exist at all. In general, the solution function can be written as

$$\phi = \phi_o(r, \theta) + \phi_s(r, \theta) \quad (11)$$

where

$$\phi_o(r, \theta) = \begin{cases} \phi_i + \phi_r & \pi - \alpha > \theta > 0 \\ \phi_i & \pi + \alpha > \theta > \pi - \alpha \\ 0 & \theta_o > \theta > \pi + \alpha \end{cases} \quad (12)$$

The equation reveals that  $\phi_o$  is the sum of the incident and reflected waves  $\phi_i$  and  $\phi_r$  and is a known function. The scattered wave  $\phi_s$  is the only unknown function to be determined in the problem. Nevertheless, the total wave  $\phi$  instead of the scattered wave  $\phi_s$  is the desired solution to be obtained in this study.

12. The solution for the total wave  $\phi$  is pursued. The finite cosine transform of  $\phi$ , denoted by  $\bar{\phi}$ , is introduced by the formula

$$\bar{\phi}(kr, n) = \int_0^{\nu\pi} \phi(kr, \theta) \cos \frac{n\theta}{\nu} d\theta \quad (13)$$

where  $n = 0, 1, 2, \dots$  are integers, and  $\nu$  is related to the wedge angle as defined by

$$\theta_o = \nu\pi \quad (14)$$

Applying the finite cosine transform and using the boundary condition in Equation 5, Equation 2 becomes

$$r^2 \frac{\partial^2 \bar{\phi}}{\partial r^2} + r \frac{\partial \bar{\phi}}{\partial r} + \left[ (kr)^2 - \left( \frac{n}{\nu} \right)^2 \right] \bar{\phi} = 0 \quad (15)$$

Equation 15 is a form of the Bessel equation for which general solutions are the Bessel functions of the first and second kinds,  $J_{n/\nu}(kr)$  and  $Y_{n/\nu}(kr)$ , respectively. Since  $Y_{n/\nu}(kr)$  are singular at the origin, the solution is chosen to be

$$\bar{\phi}(kr, n) = a_n J_{n/v}(kr) \quad (16)$$

where  $a_n$  are constants to be determined.

13. Taking the finite cosine transform of Equation 11 and using Equation 16, we have

$$\int_0^{v\pi} \phi_s \cos \frac{n\theta}{v} d\theta = a_n J_{n/v}(kr) - \int_0^{v\pi} \phi_o \cos \frac{n\theta}{v} d\theta \quad (17)$$

or

$$\bar{\phi}_s = a_n J_{n/v}(kr) - \bar{\phi}_o \quad (18)$$

Then applying the operation  $\lim_{r \rightarrow \infty} \sqrt{r}(\partial/\partial r + ik)$  to both sides of Equation 18, and using the Sommerfeld radiation condition (Equation 6) we have

$$\lim_{r \rightarrow \infty} \sqrt{r} \left( \frac{\partial}{\partial r} + ik \right) \left[ a_n J_{n/v}(kr) - \int_0^{v\pi} \phi_o \cos \frac{n\theta}{v} d\theta \right] = 0 \quad (19)$$

14. Equation 19 can be asymptotically evaluated to determine  $a_n$ . Firstly, the first term involving the Bessel function is evaluated. The function  $J_{n/v}(kr)$  at  $r \rightarrow \infty$  behaves asymptotically (Abramowitz and Stegun 1964) as follows:

$$J_{n/v}(kr) \sim \sqrt{\frac{2}{\pi kr}} \cos \left( kr - \frac{n\pi}{2v} - \frac{\pi}{4} \right) \quad (20)$$

Hence, we have

$$\lim_{r \rightarrow \infty} \sqrt{r} \left( \frac{\partial}{\partial r} + ik \right) J_{n/v}(kr) \sim \sqrt{\frac{2k}{\pi}} e^{i(kr - n\pi/2v + \pi/4)} \quad (21)$$

Secondly, the second term involving the integral of  $\phi_0$  is evaluated. The asymptotic behavior of the integral over  $\theta = (0, \nu\pi)$  and at large distance  $r \rightarrow \infty$  can be found by the method of stationary phase. The integral, after substituting  $\phi_0$  from Equations 9, 10, and 12, can be written as

$$\int_0^{\nu\pi} \phi_0 \cos \frac{n\theta}{\nu} d\theta = \int_0^{\pi-\alpha} \left[ e^{ikr \cos(\theta-\alpha)} + e^{ikr \cos(\theta+\alpha)} \right] \cos \frac{n\theta}{\nu} d\theta \\ + \int_{\pi-\alpha}^{\pi+\alpha} e^{ikr \cos(\theta-\alpha)} \cos \frac{n\theta}{\nu} d\theta \quad (22)$$

In the integrals, there are three points of stationary phase at  $\theta = \alpha$  and  $\theta = \pi \pm \alpha$ . If the same argument as that of Stoker (1957) is followed, of the three contributions only the first one  $\theta = \alpha$  furnishes a nonvanishing contribution for  $r \rightarrow \infty$  when the operator  $\sqrt{r}(\partial/\partial r + ik)$  is applied to it. The physical significance of this statement is that only the incident wave is effective in determining the cosine coefficients of the solution. Therefore,

$$\lim_{r \rightarrow \infty} \sqrt{r} \left( \frac{\partial}{\partial r} + ik \right) \int_0^{\nu\pi} \phi_0 \cos \frac{n\theta}{\nu} d\theta \sim 2\sqrt{2\pi k} \cos \frac{n\alpha}{\nu} e^{i(kr+\pi/4)} \quad (23)$$

Substituting Equations 21 and 23 into Equation 19, we obtain the unknown coefficients  $a_n$ :

$$a_n = 2\pi \cos \frac{n\alpha}{\nu} e^{in\pi/2\nu} \quad (24)$$

15. Since the solution  $\phi$  in the cosine series expression is

$$\phi(r, \theta) = \frac{1}{\nu\pi} \bar{\phi}(r, 0) + \frac{2}{\nu\pi} \sum_{n=1}^{\infty} \bar{\phi}(r, n) \cos \frac{n\theta}{\nu} \quad (25)$$

the solution is obtained by substituting Equations 16 and 24 into Equation 25 as follows:

$$\phi(r, \theta) = \frac{2}{v} \left[ J_0(kr) + 2 \sum_{n=1}^{\infty} e^{in\pi/2v} J_{n/v}(kr) \cos \frac{n\alpha}{v} \cos \frac{n\theta}{v} \right] \quad (26)$$

Equation 26 is the solution for the combined wave reflection and diffraction by a vertical wedge of arbitrary wedge angle and is considered to be extended from the solution by Stoker (1957) who only solved the problem of a thin semi-infinite breakwater. The solution in Equation 26 and the one by Stoker are not only in nonclosed form but also in terms of Bessel functions. It seems that the calculations of the solutions are very difficult without using a modern high-speed computer. This is probably the reason why Stoker arrived at his solution expressed in the same cosine series but did not use it to calculate the result. Instead, he further transformed the expression into a very complex integral form for further approximation in calculating the result.

16. Notably, the solution at the origin point is obtained by simply substituting  $r = 0$  into Equation 26 to arrive at

$$\phi(0, \theta) = \frac{2}{v} \quad (27)$$

Therefore, wave response at the origin point depends only on the wedge angle and does not depend on the incident wave angle.

#### Two Special Cases

17. The solutions for two special cases are used to verify Equation 26: one for the case of a thin semi-infinite breakwater and the other for the case of an infinite wall extending from  $x = -\infty$  to  $\infty$ .

18. The vertical wedge should reduce to a thin semi-infinite breakwater as the wedge angle reduces to 0 deg. Therefore, solution of the combined wave reflection and diffraction by a thin semi-infinite breakwater is obtained by substituting  $v = 2$  (that is,  $\theta_0 = 2\pi$ ) into Equation 26 which then becomes

$$\phi(r, \theta) = J_0(kr) + 2 \sum_{n=1}^{\infty} e^{in\pi/4} J_{n/2}(kr) \cos \frac{n\alpha}{2} \cos \frac{n\theta}{2} \quad (28)$$

Equation 28 is precisely the same one obtained by Stoker (1957).

19. The vertical wedge should also become an infinite wall extending from  $x = -\infty$  to  $\infty$  with the water occupying only the half plane of  $y \geq 0$  as the wedge angle increases to 180 deg. In this situation the scattered wave is absent from the solution, and the total wave is only the sum of the incident and reflected waves as follows:

$$\phi(r, \theta) = e^{ikr \cos(\theta-\alpha)} + e^{ikr \cos(\theta+\alpha)} \quad (29)$$

After expansion of the exponential functions in terms of Bessel functions (Abramowitz and Stegun 1964), Equation 29 becomes

$$\phi(r, \theta) = 2 \left[ J_0(kr) + 2 \sum_{n=1}^{\infty} i^n J_n(kr) \cos n\alpha \cos n\theta \right] \quad (30)$$

Equation 30 is the same equation reduced from Equation 26 by substituting  $\nu = 1$  into it.

### PART III: CALCULATION AND RESULTS

20. Results of the combined reflection and diffraction by a wedge of arbitrary wedge angle can be calculated from Equation 26. Since the solution is not only in terms of Bessel functions but also in a nonclosed form, the computer program WEDGE is therefore written to calculate the solution.

21. In the program the subroutine BESJ for calculating Bessel function of fractional or integer order was used. The subroutine was originally written by Amos, Daniel, and Weston in 1975 (Morris 1984) and is collected in the Naval Surface Weapons Center Library of Mathematics Subroutines (Morris 1984).

22. In the calculation the summation of the infinite terms in Equation 26 was carried out to the term which is preceded by eight successive terms of the absolute value of the Bessel function, all equal to or less than  $10^{-8}$ . The solution has a truncation error less than  $10^{-8}$ , and it is of the order of one.

23. In this study, results of the combined wave reflection and diffraction for the wedge are calculated for two cases: one for a vertical wedge of 0-deg wedge angle and the other for a vertical wedge of 90-deg wedge angle.

#### Vertical Wedge of 0-Deg Wedge Angle

24. When the wedge angle is equal to zero, the wedge is actually a thin semi-infinite breakwater extending from  $x = 0$  to  $\infty$ . Figure 3 shows the thin semi-infinite breakwater along with the polar coordinates. In this case the diffraction results for various incident wave angles in the water region from  $\theta = \pi$  to  $2\pi$  and  $r/\lambda \leq 10$ , where  $\lambda$  is the incident wave length, have already been presented by Wiegel (1962) and are shown in the SPM, Volume I (1984). The present results combine reflection and diffraction effects and cover the water region from  $\theta = 0$  to  $2\pi$  and  $r/\lambda \leq 10$ . Therefore, the present results for this particular case can be considered to be a complementary and extended version to the ones in the SPM.

25. In this study wave response was calculated at 1,460 grid points intersected by  $r/\lambda = 0.5, (0.5), 10$ , which means that the values of  $r/\lambda$  are from 0.5 to 10.0 with each value increment being 0.5. Hereafter, all similar expressions are to be interpreted in the same way (e.g.,  $\theta = 0, (\pi/36), 2\pi$  for

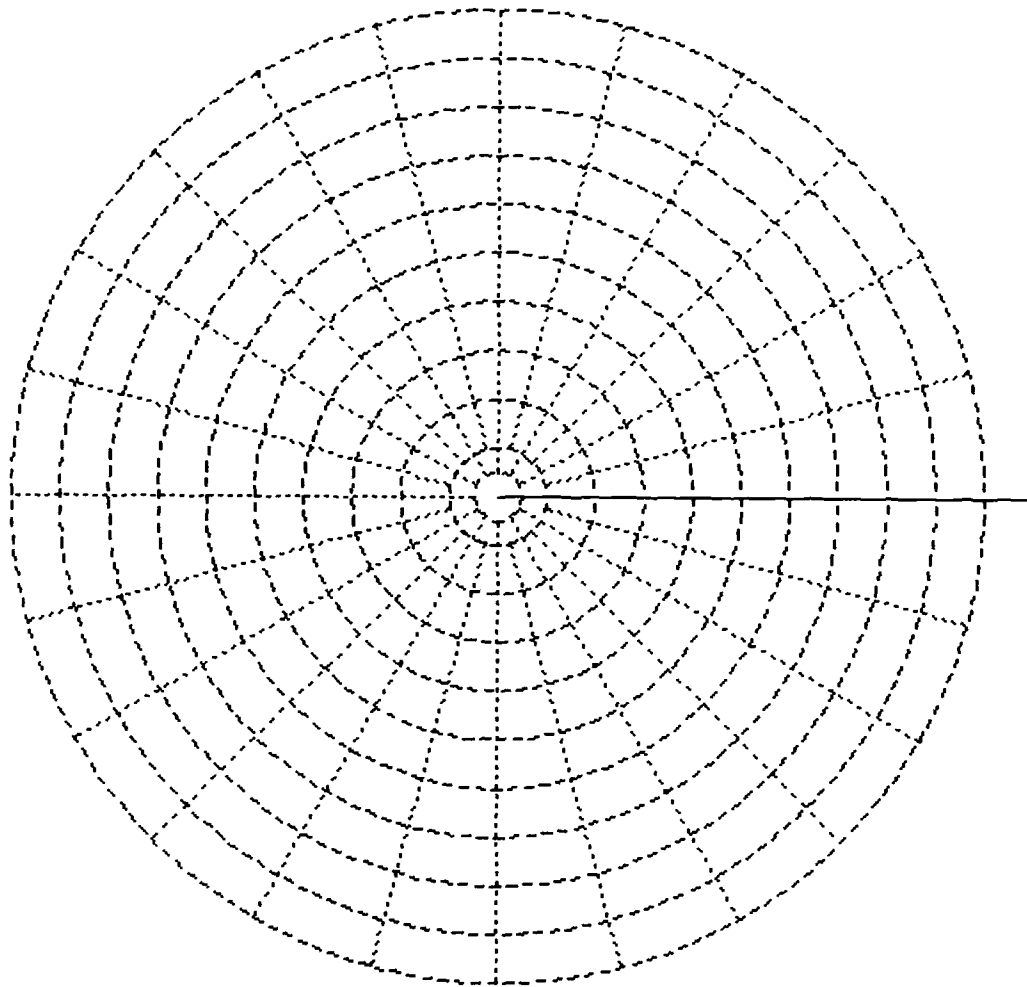


Figure 3. Thin semi-infinite breakwater and polar coordinates  
the incident wave angle  $\alpha = 0, (\pi/12), \pi$  . The wave response at the origin  
point is obtained substituting  $\nu = 2$  into Equation 27, as follows:

$$\phi(0, \theta) = 1 \quad (31)$$

Those calculated values were used to interpret the value for each non-overlapping pixel of size  $0.1r/\lambda$  by  $0.1r/\lambda$  in the area within the  $10r/\lambda$  radius from the origin. A diagram was then constructed by patching those pixels over the entire area. The wave response diagrams for each incident wave angle are shown in Figures 4 through 15. Notably, the values in the diagrams constitute the amplification factor which is defined as the ratio of the total wave height to the incident wave height. Therefore, in subregions II

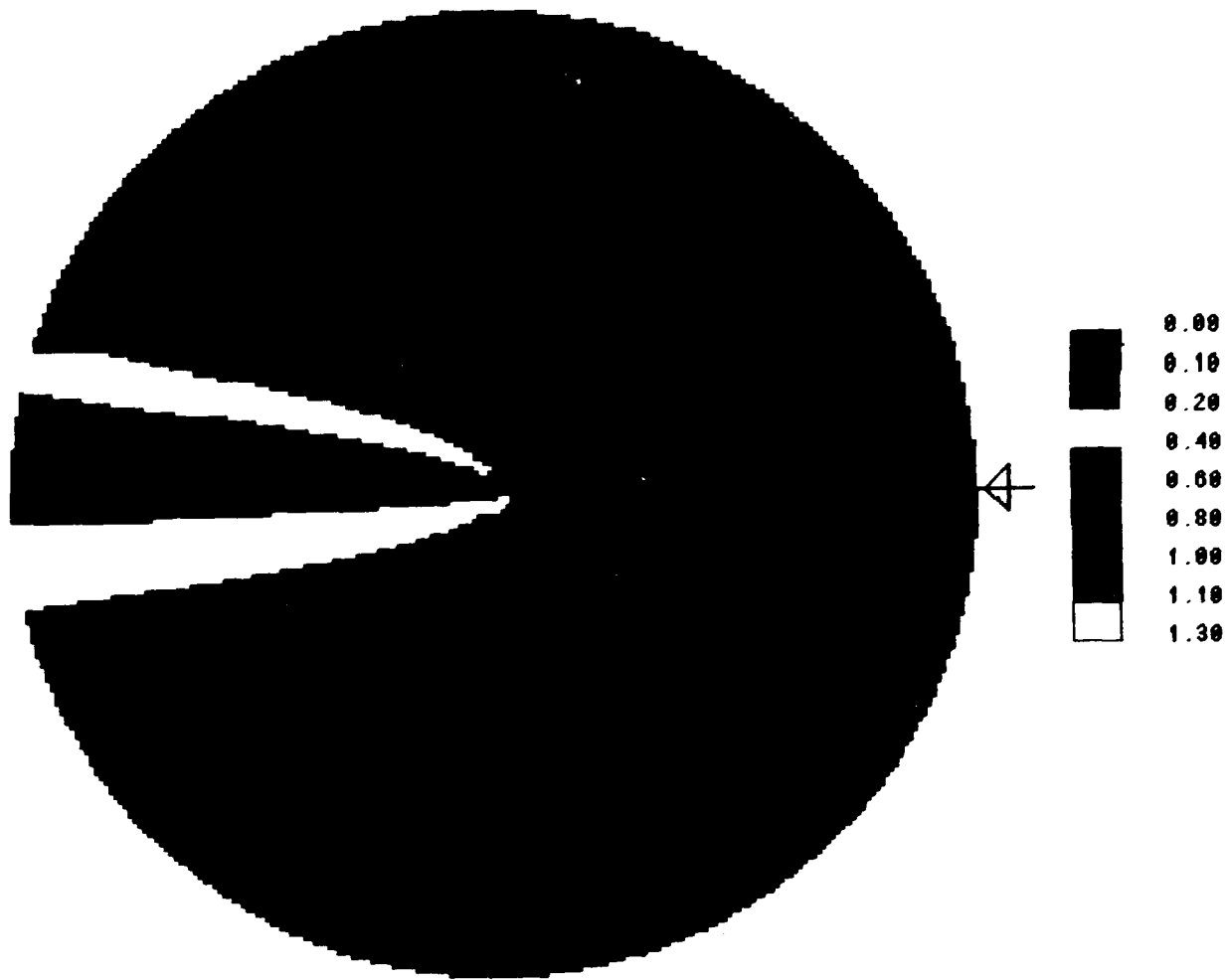


Figure 4. Amplification factor diagram for the thin semi-infinite breakwater for incident wave angle = 0 deg

and III (as defined in Figure 2) where the reflected wave is absent, the amplification factor is essentially the diffraction coefficient as defined in the SPM.

26. Figures 4 through 15 reveal that the amplification factors in sub-region I change very rapidly between 0 and 2.35 over the subregion, and the diagram patterns become very complex because of the interesting superposition of the incident, reflected, and scattered waves. (In the legend of Figures 4 through 15, the width of the pixel is one incident wave length, and the values are amplification factors.) Such patterns would be very difficult to construct without using a high-speed computer and computer graphics. In sub-regions II and III, the amplification factors change smoothly from 1.15 roughly along the reflected wave ray reflected from the origin point to nearly

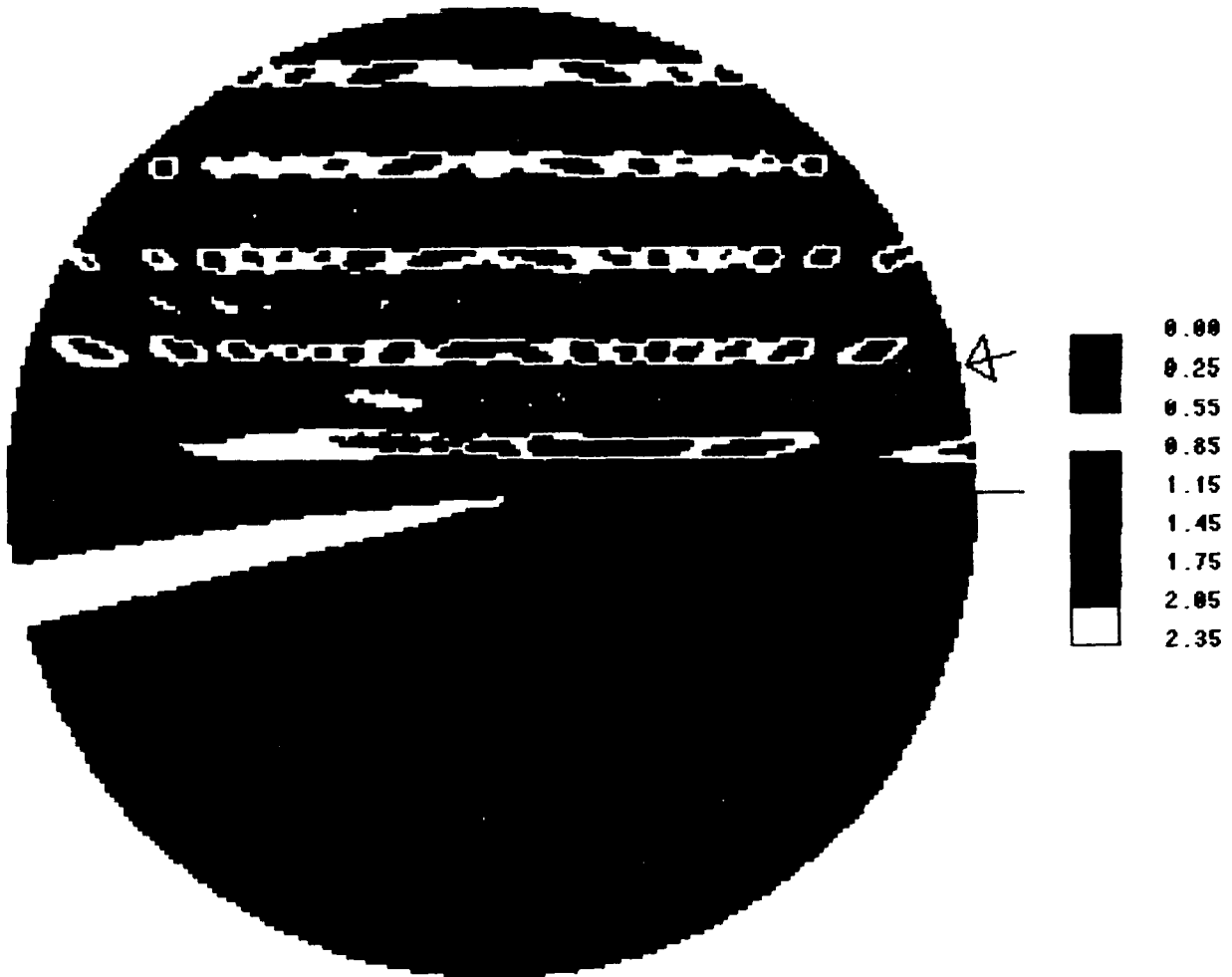


Figure 5. Amplification factor diagram for the thin semi-infinite breakwater for incident wave angle = 15 deg

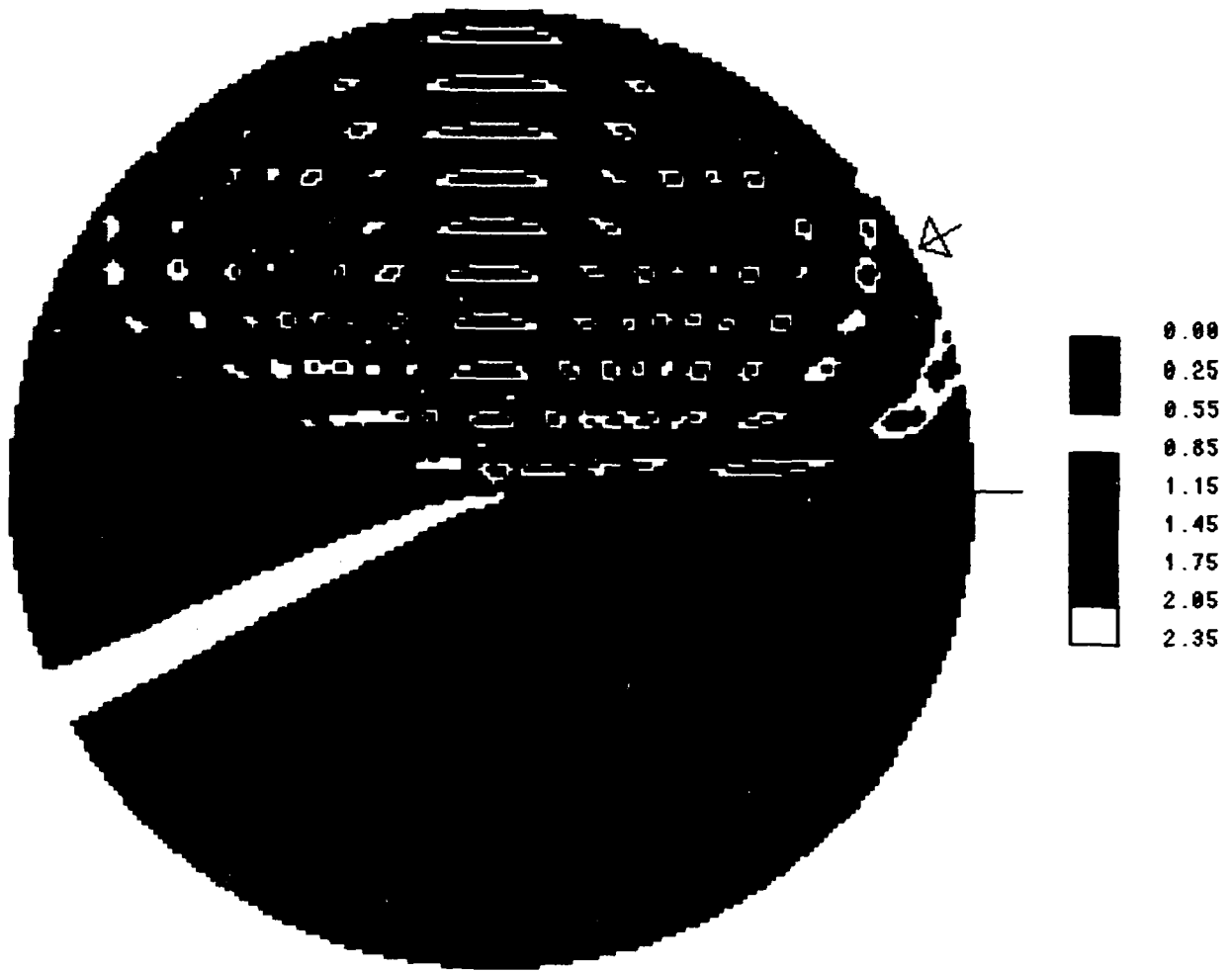


Figure 6. Amplification factor diagram for the thin semi-infinite breakwater for incident wave angle = 30 deg



Figure 7. Amplification factor diagram for the thin semi-infinite breakwater for incident wave angle = 45 deg

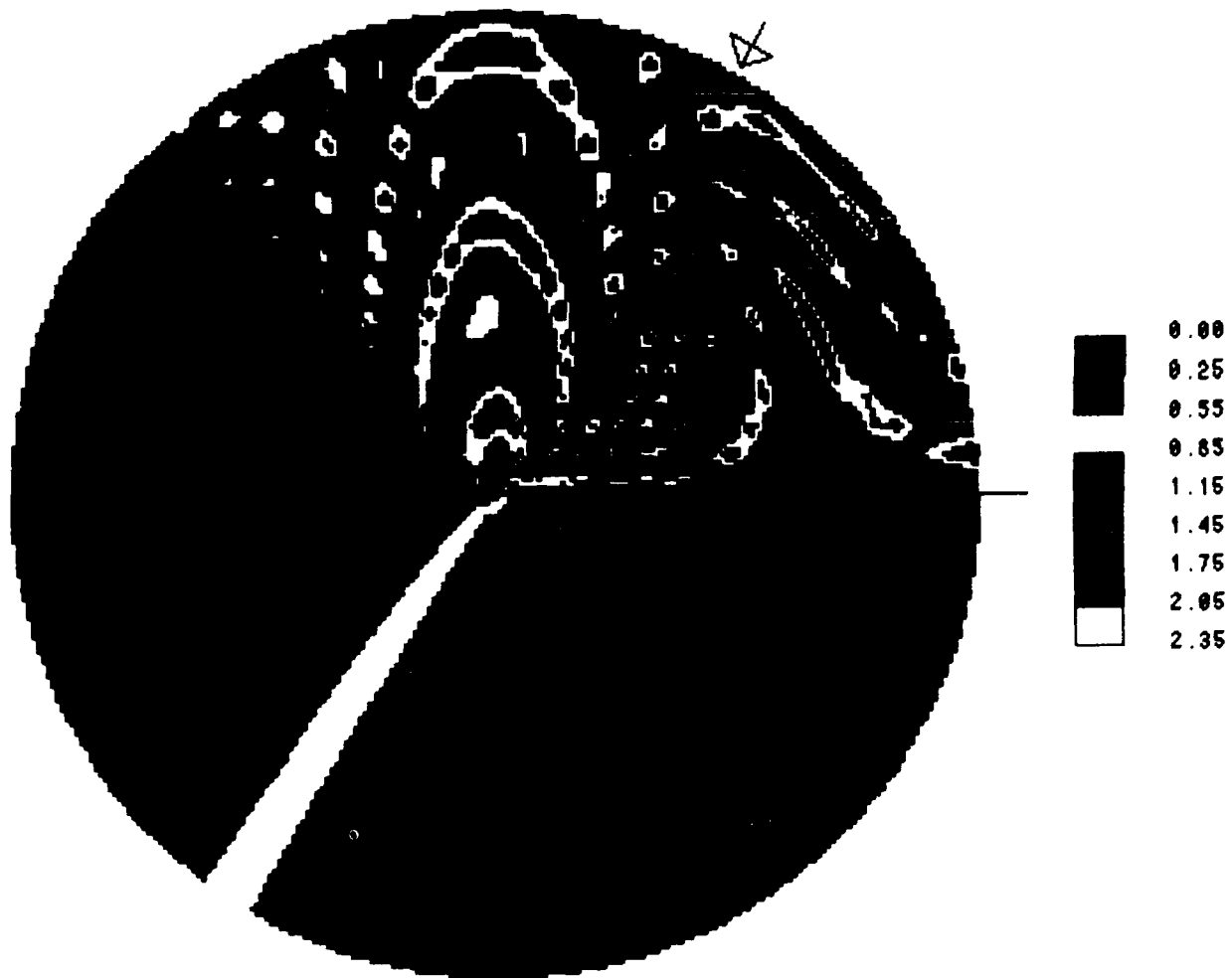


Figure 8. Amplification factor diagram for the thin semi-infinite breakwater for incident wave angle = 60 deg



Figure 9. Amplification factor diagram for the thin semi-infinite breakwater for incident wave angle = 75 deg

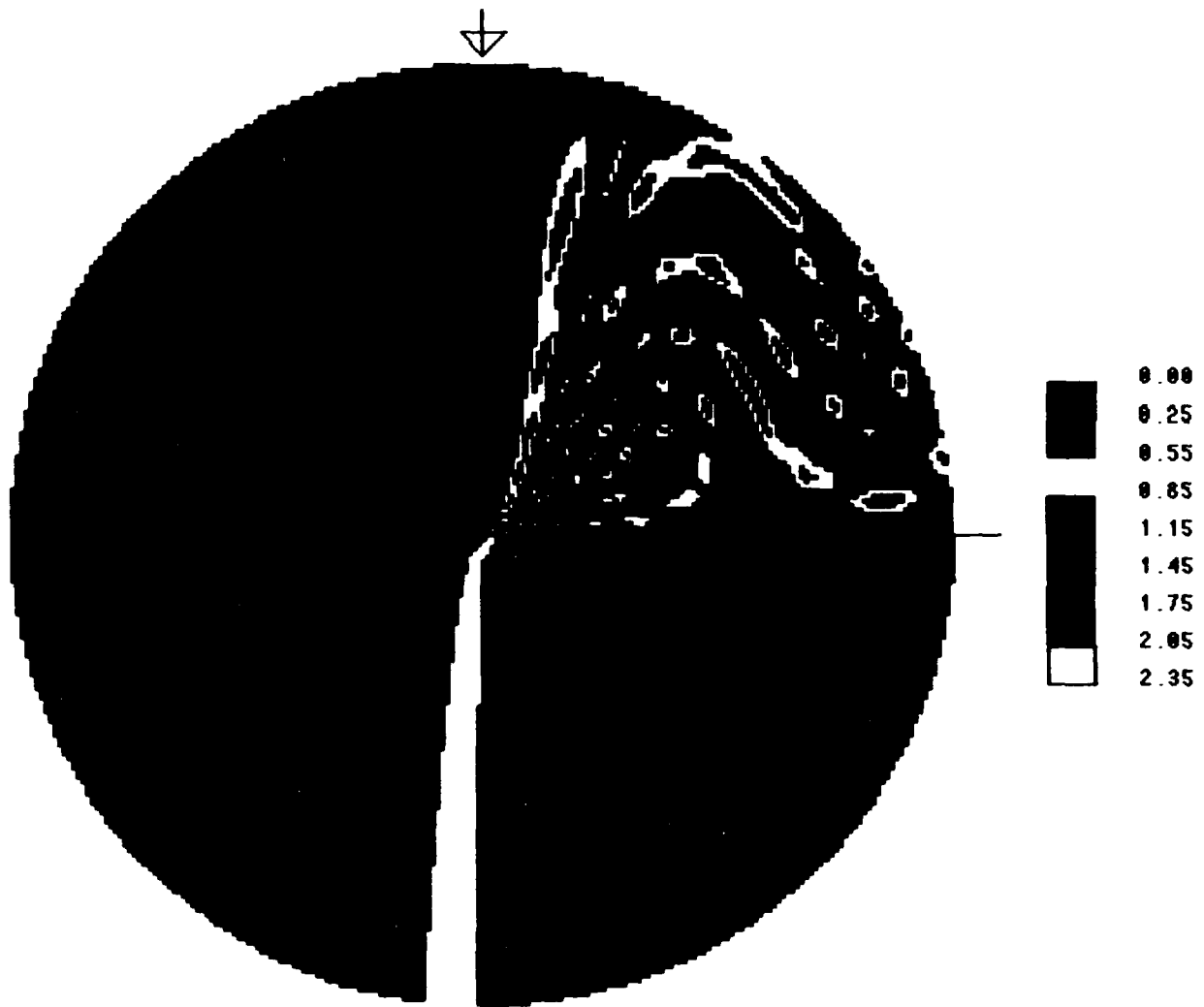


Figure 10. Amplification factor diagram for the thin semi-infinite breakwater for incident wave angle  $\approx 90$  deg

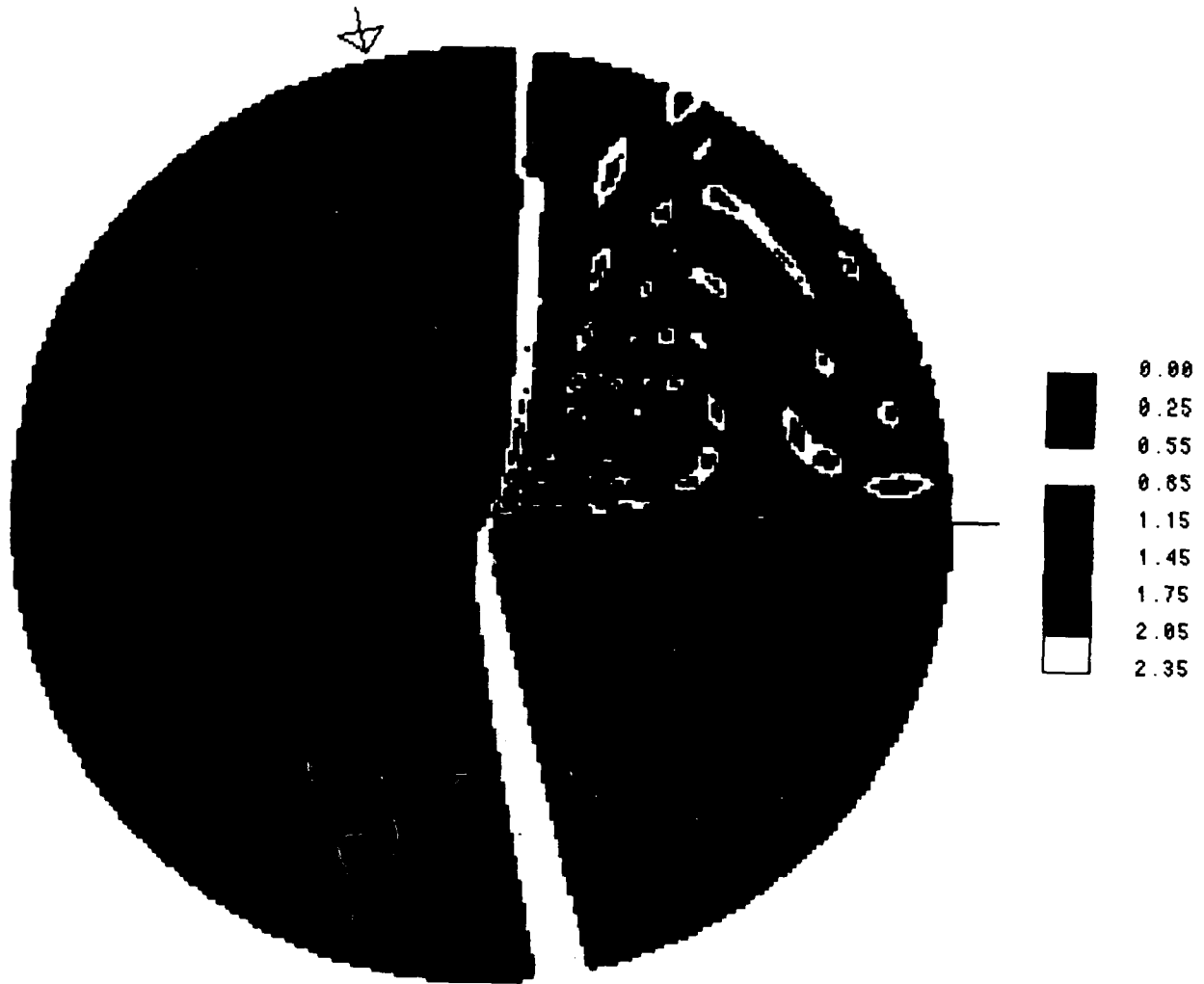


Figure 11. Amplification factor diagram for the thin semi-infinite breakwater for incident wave angle = 105 deg



Figure 12. Amplification factor diagram for the thin semi-infinite breakwater for incident wave angle = 120 deg

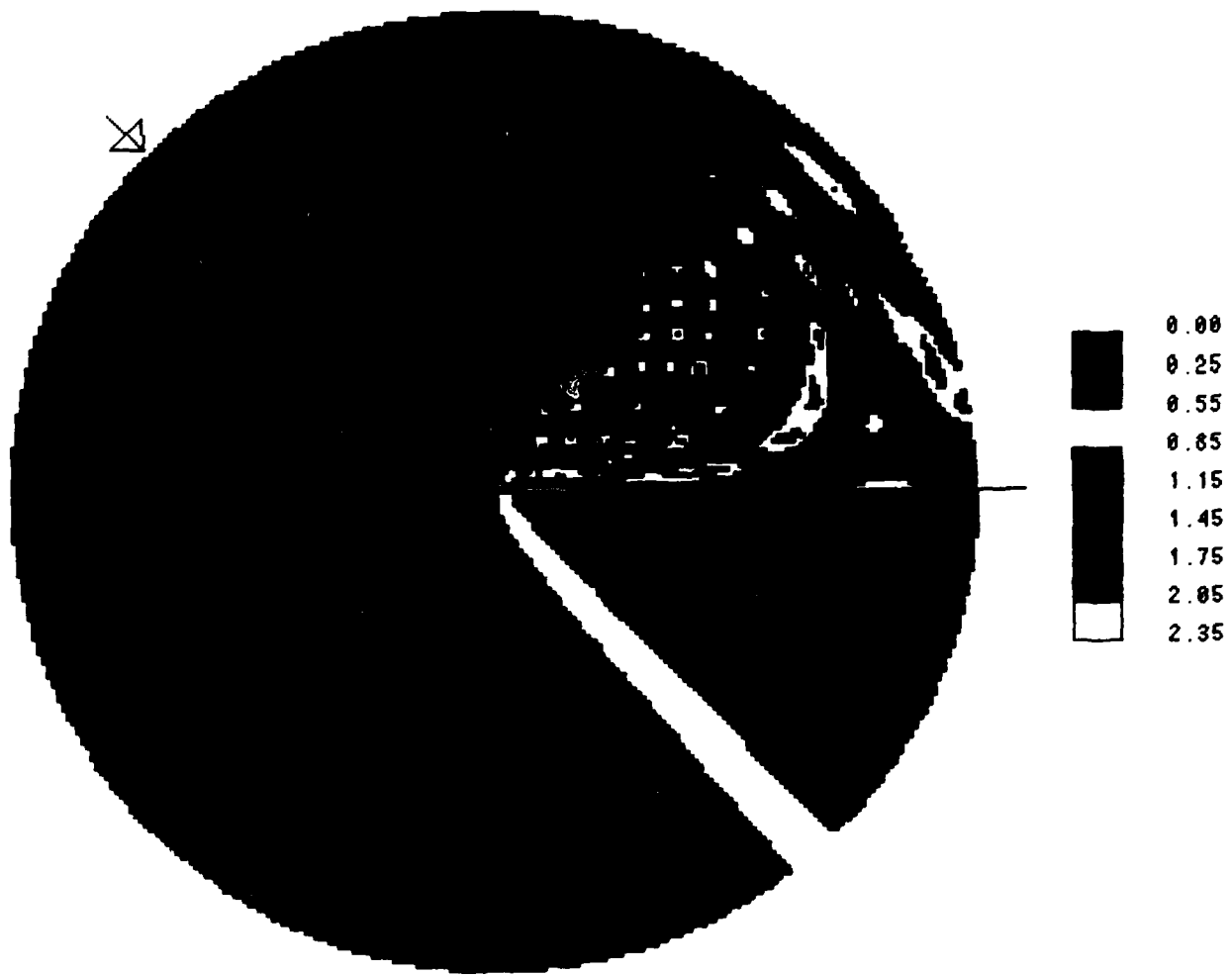


Figure 13. Amplification factor diagram for the thin semi-infinite breakwater for incident wave angle = 135 deg



Figure 14. Amplification factor diagram for the thin semi-infinite breakwater for incident wave angle = 150 deg



Figure 15. Amplification factor diagram for the thin semi-infinite breakwater for incident wave angle = 165 deg

0.00 at the back wall of the wedge in the shadow zone. The diagram patterns are relatively smooth and simple.

27. Notably, the diagrams do not include phase information of the wave response which is usually unimportant in most engineering practice. Should the phase of the wave response need to be known, one can always use the computer program WEDGE to calculate it.

28. The contour diagrams of the amplification factor, similar to the ones presented by Wiegel (1962) and shown in the SPM (1984), were also plotted as typically shown in Figure 16. Examination of those contour diagrams indicates that, in subregion III, the results are identical to Wiegel's results. But in subregion II the contour patterns for the amplification factor (or the diffraction coefficient  $K'$  used in the SPM (1984)) equal to 1.0; thus the present results are far more complicated than Wiegel's. The author believes that Wiegel's results may lose accuracy because of insufficient resolution of the computational tools during the late fifties and early sixties. Nevertheless, such inaccuracies are usually either tolerable or immaterial in most engineering practice.

29. The contour patterns in subregion I are very complex, and it is difficult to track specific contours. Therefore, for clarity only the patched diagrams are presented, and the contour diagrams are omitted in this report.

#### Vertical Wedge of 90-Deg Wedge Angle

30. When the wedge angle is equal to  $\pi/2$  ( $\theta_0 = 3\pi/2$ ), the vertical wedge occupies the entire fourth quadrant of the space as shown in Figure 17. Wave response was calculated at 1,100 grid points intersected at  $r/\lambda = 0.5, (0.5), 10.0$  and  $\theta = 0, (\pi/36), 3\pi/2$  for the incident wave angle  $\alpha = 0, (\pi/12), \pi$ . The wave response at the origin is obtained by substituting  $\nu = 1.5$  into Equation 27 as follows:

$$\phi(0, \theta) = \frac{4}{3} \quad (32)$$

Those calculated results were used to construct the amplification factor diagrams by following the same procedures described for the case of the thin semi-infinite breakwater. The diagrams are shown in Figures 18 through 27. Because of symmetry of the results, the diagrams for the incident wave angle  $\alpha > 3\pi/4$  can be obtained from those for an incident wave angle of  $\pi - \alpha$ .

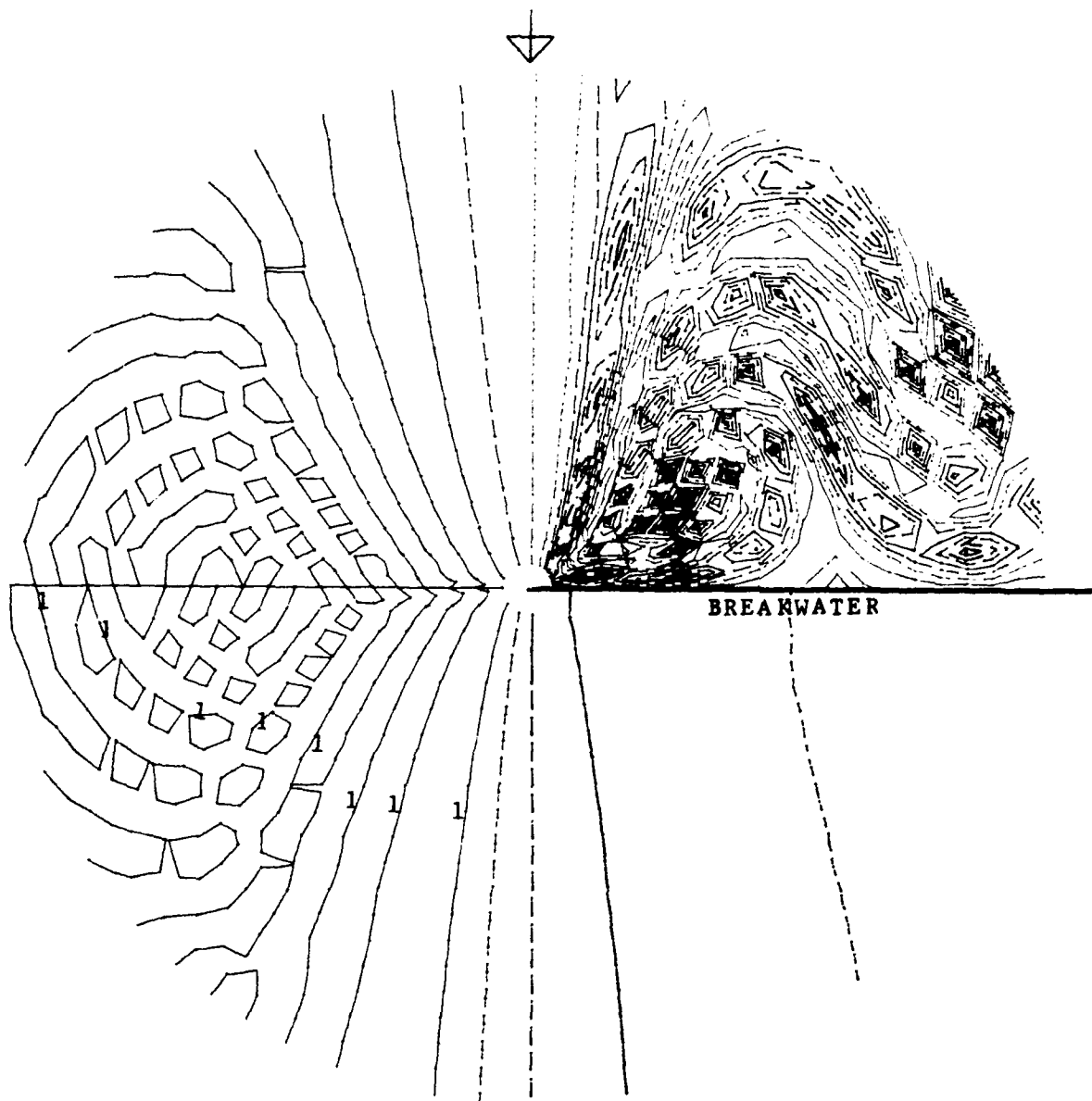


Figure 16. Amplification factor contour diagram for the thin semi-infinite breakwater for incident wave angle = 90 deg

Therefore, the diagrams for the incident wave angles  $\alpha = \pi/6, (\pi/12), \pi$  are omitted in this report.

31. The diagrams indicate that, for each corresponding incident wave angle, the results in subregion I are very similar to those obtained for the vertical wedge of 0-deg wedge angle. However, the results in subregions II and III from both wedges are discernibly different.

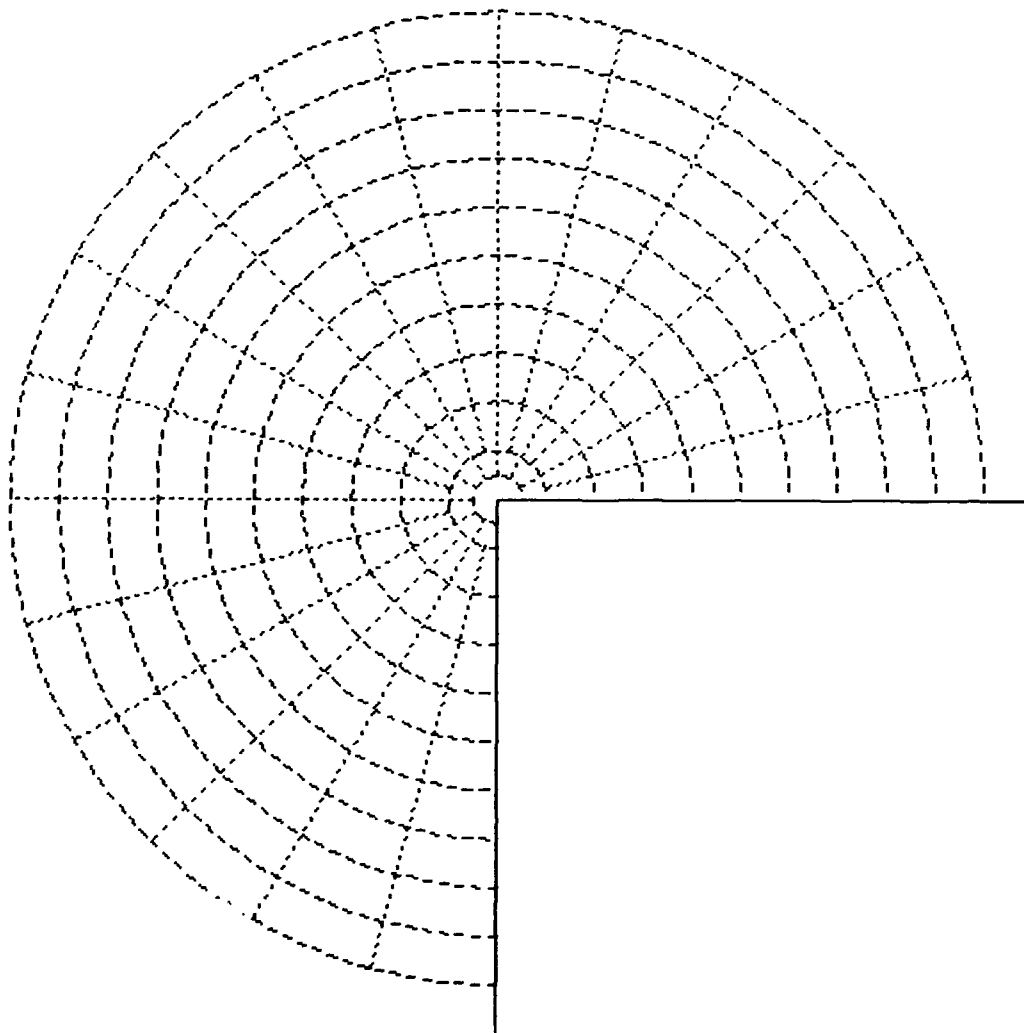


Figure 17. A 90-deg wedge and polar coordinates

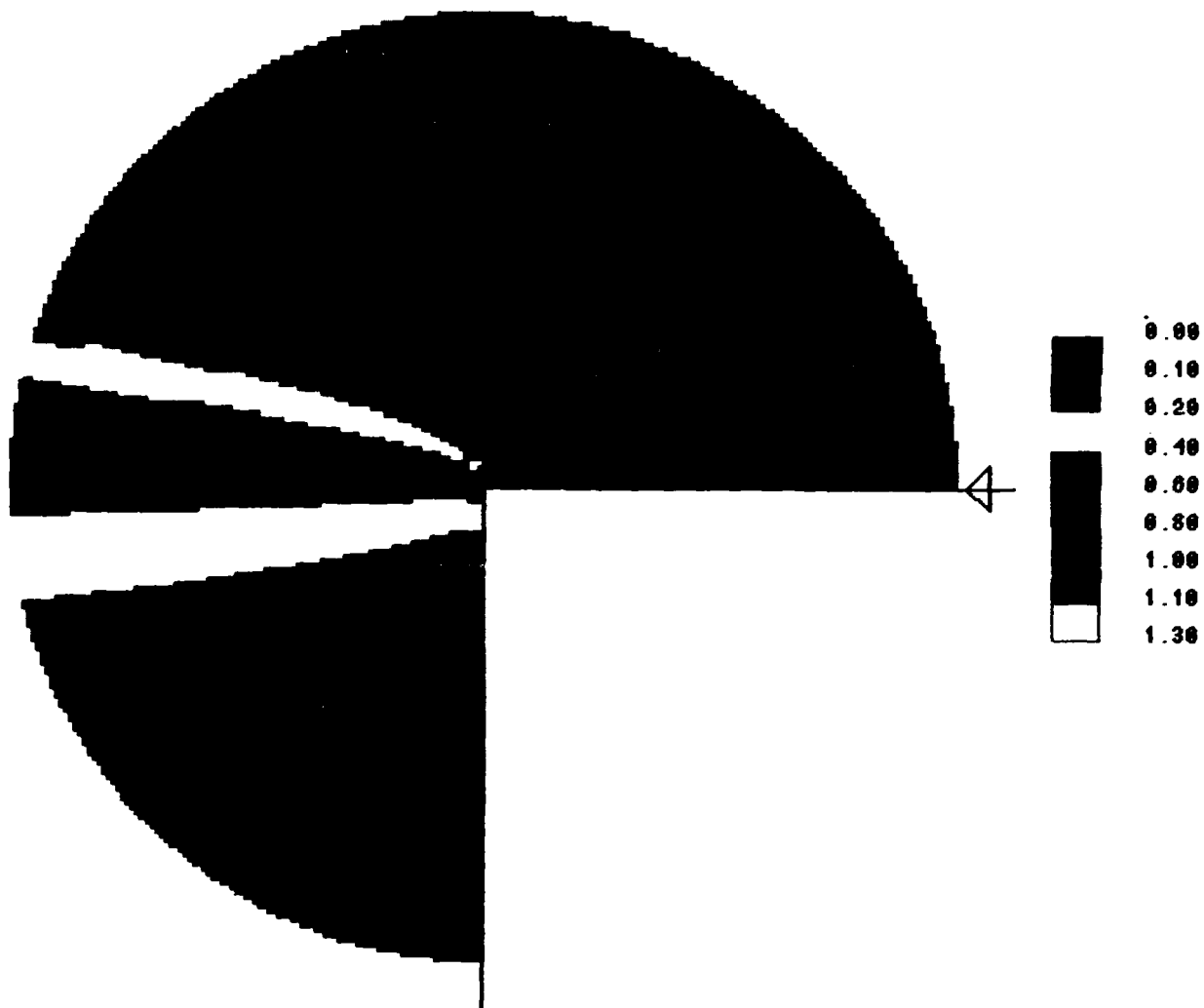


Figure 18. Amplification factor diagram for the 90-deg wedge for incident wave angle = 0 deg

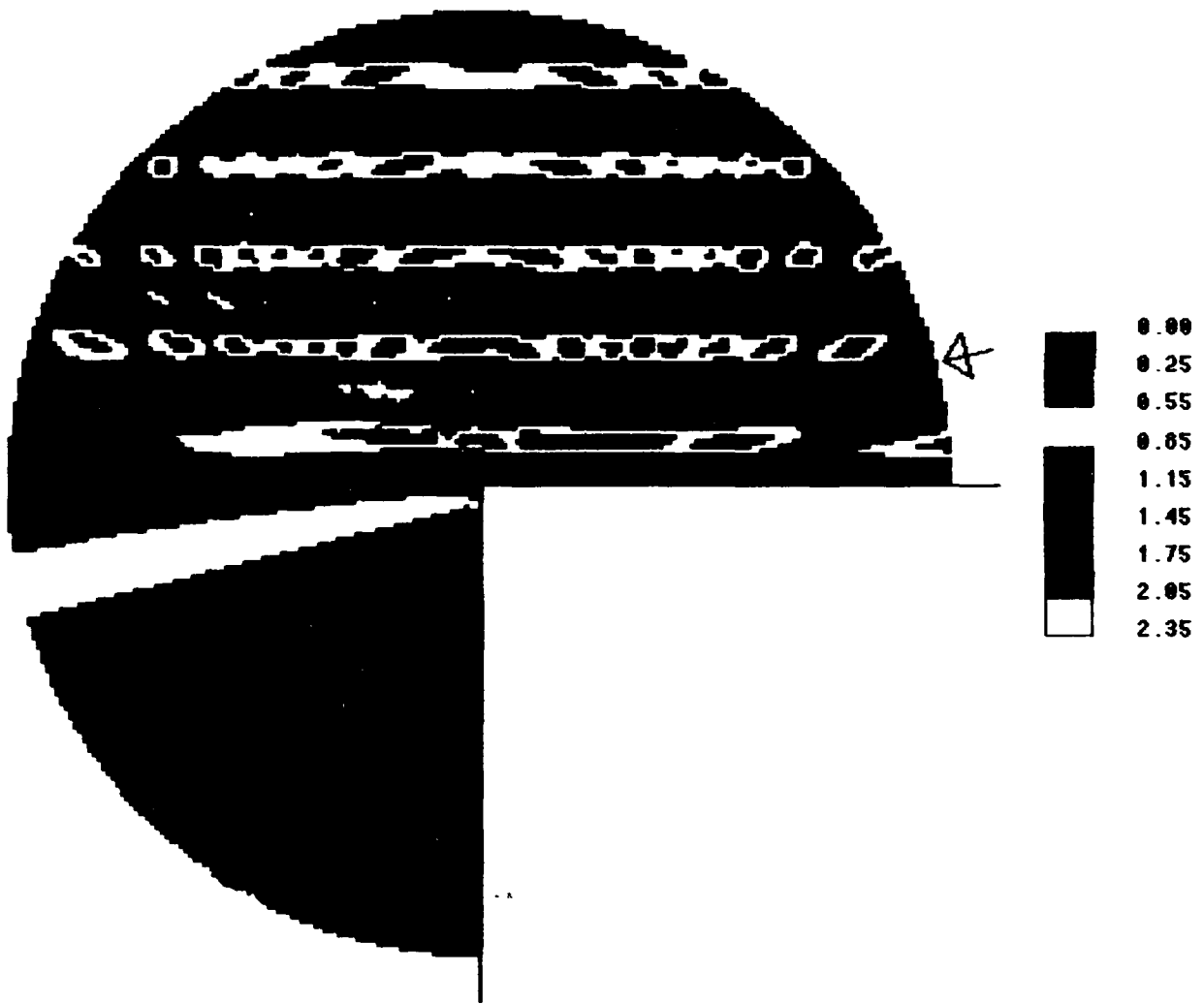


Figure 19. Amplification factor diagram for the 90-deg wedge for incident wave angle = 15 deg

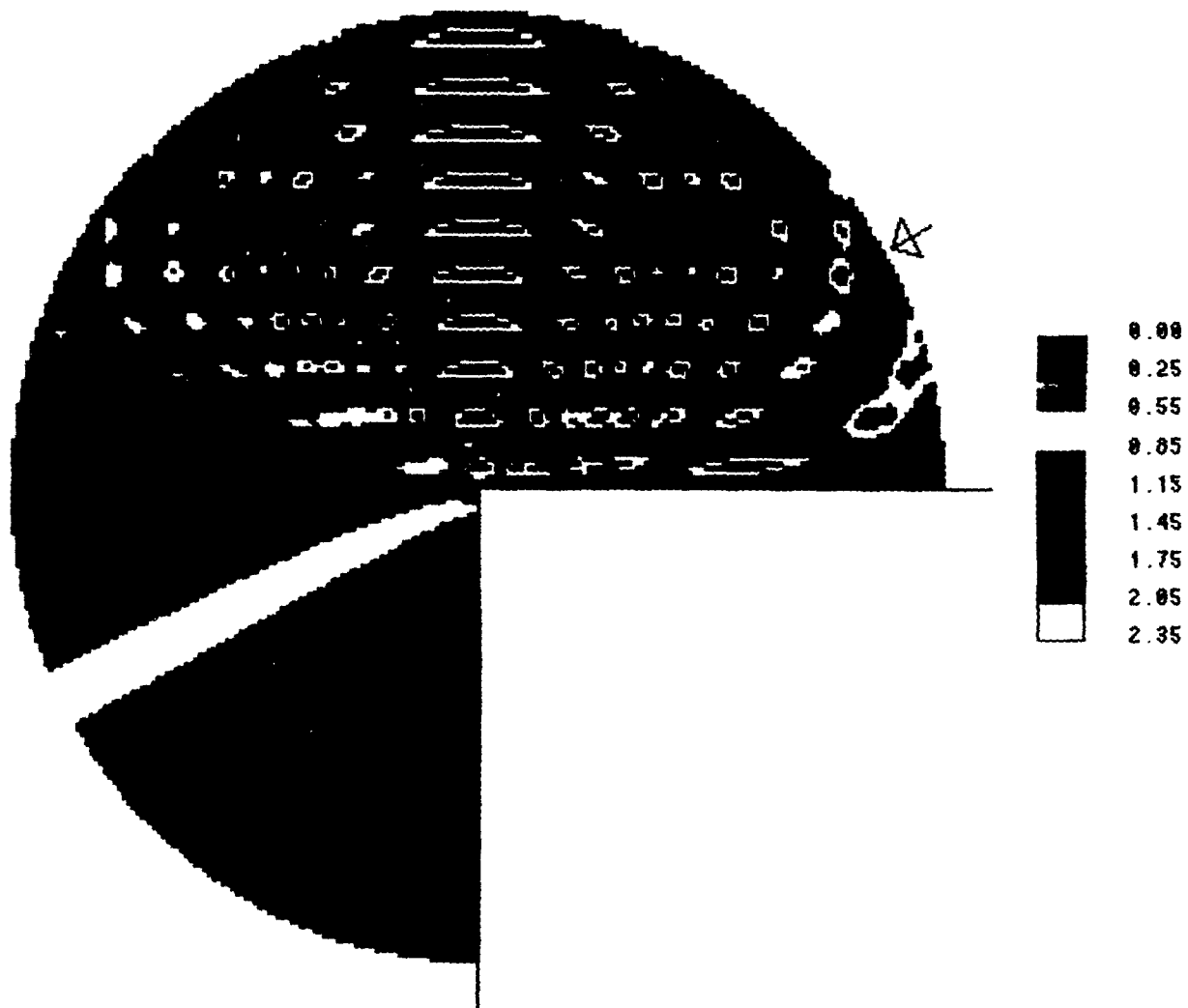


Figure 20. Amplification factor diagram for the 90-deg wedge for incident wave angle = 30 deg

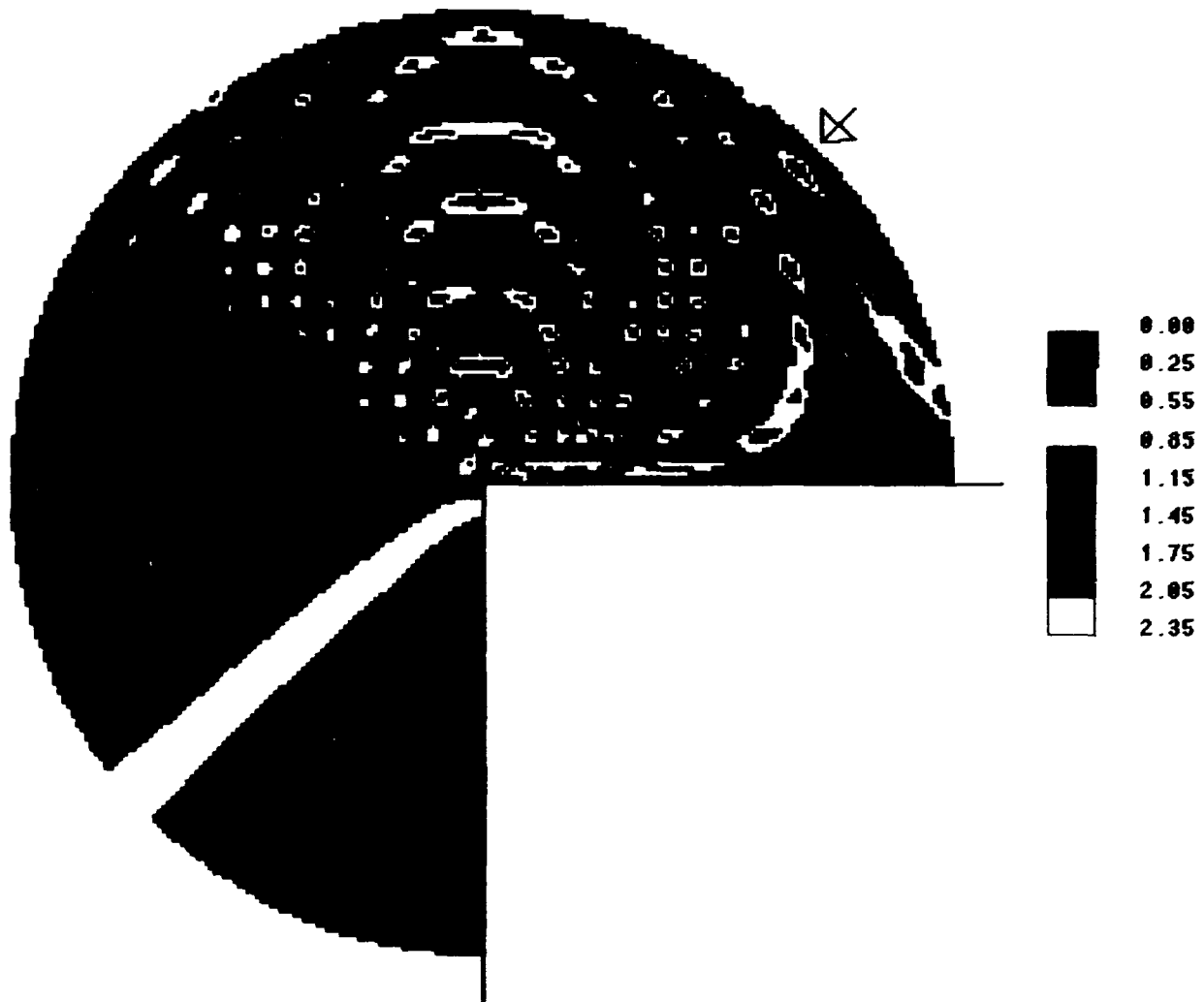


Figure 21. Amplification factor diagram for the 90-deg wedge for incident wave angle = 45 deg

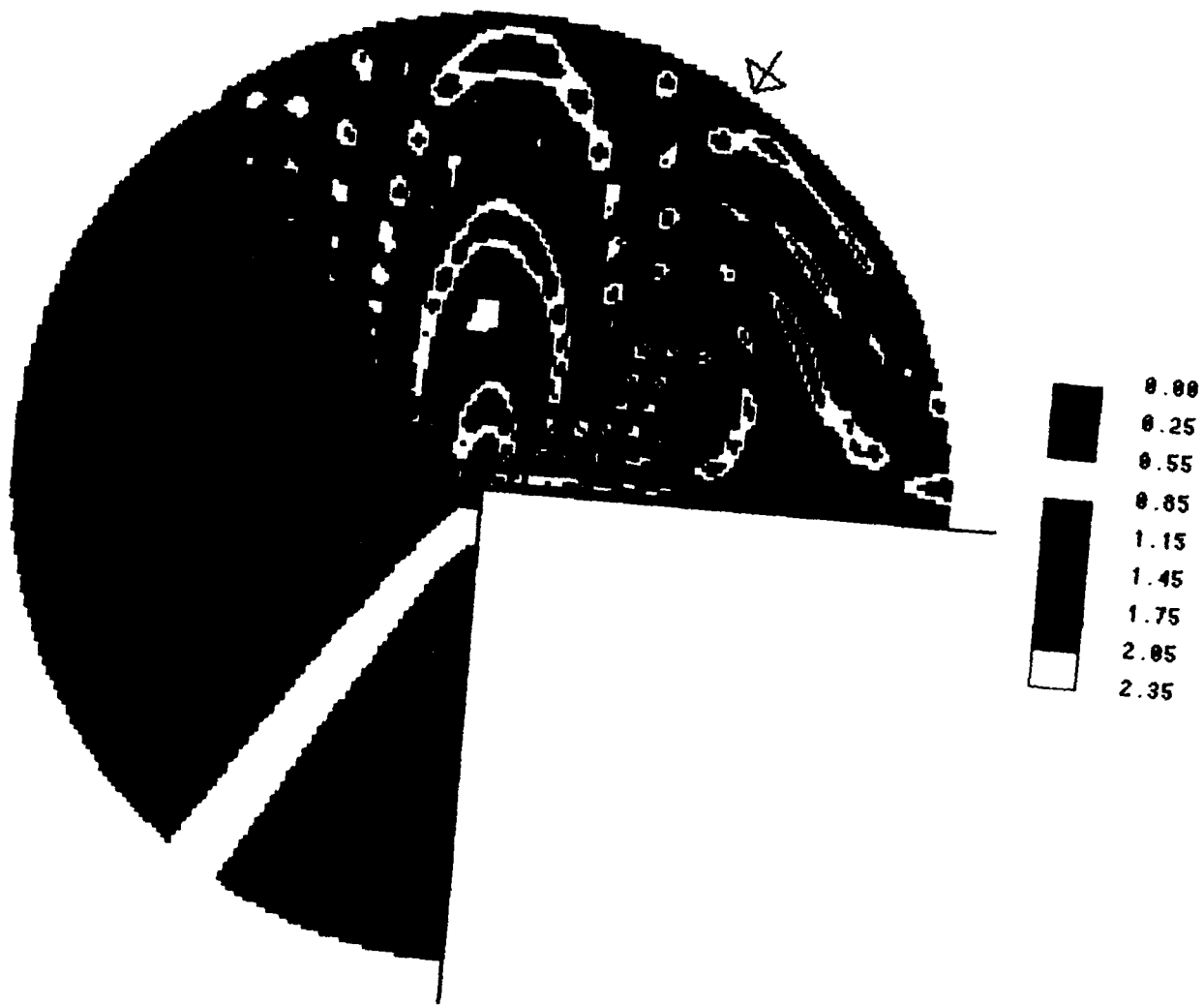


Figure 22. Amplification factor diagram for the  
90-deg wedge for incident wave angle = 60 deg

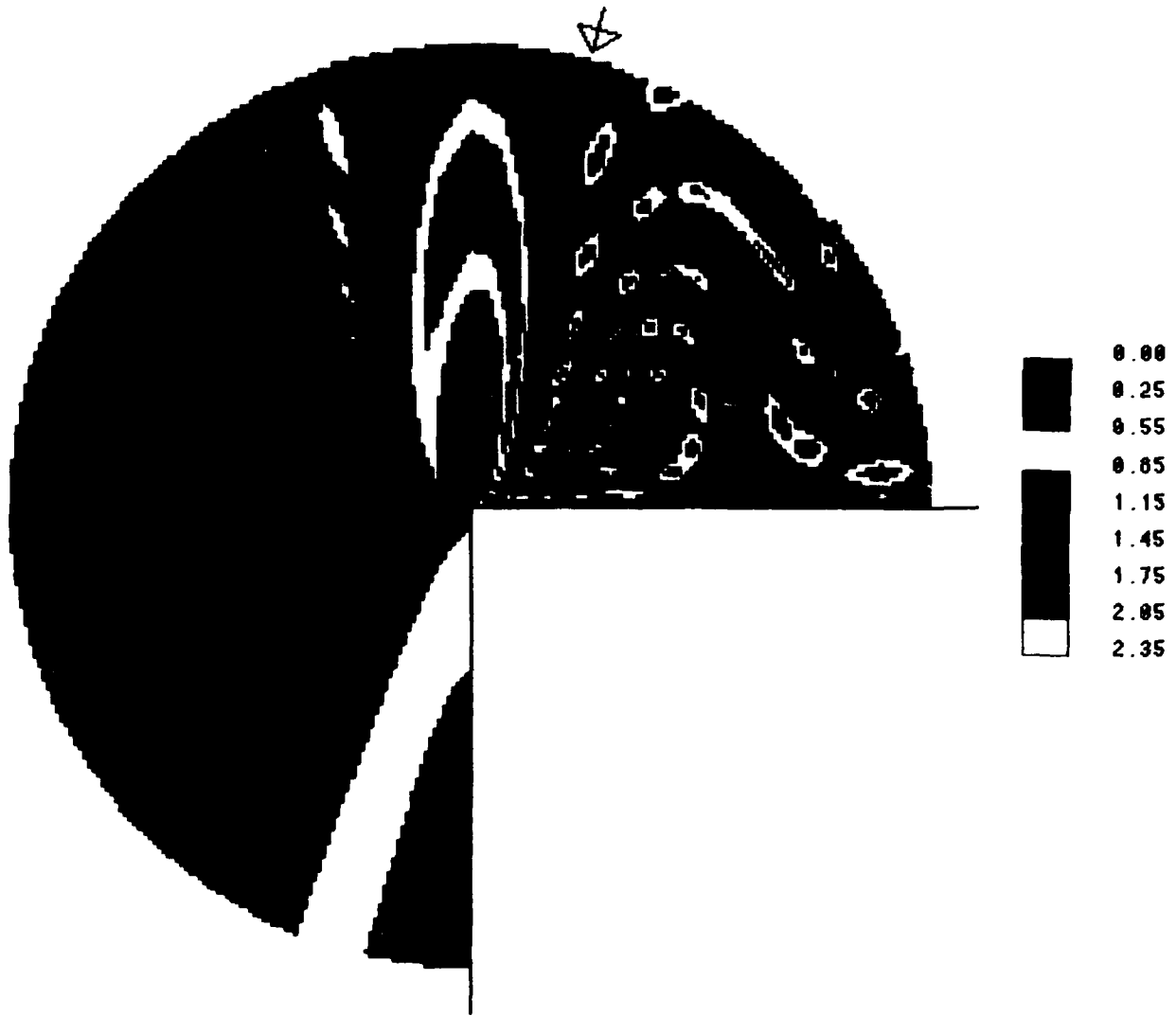


Figure 23. Amplification factor diagram for the 90-deg wedge for incident wave angle = 75 deg

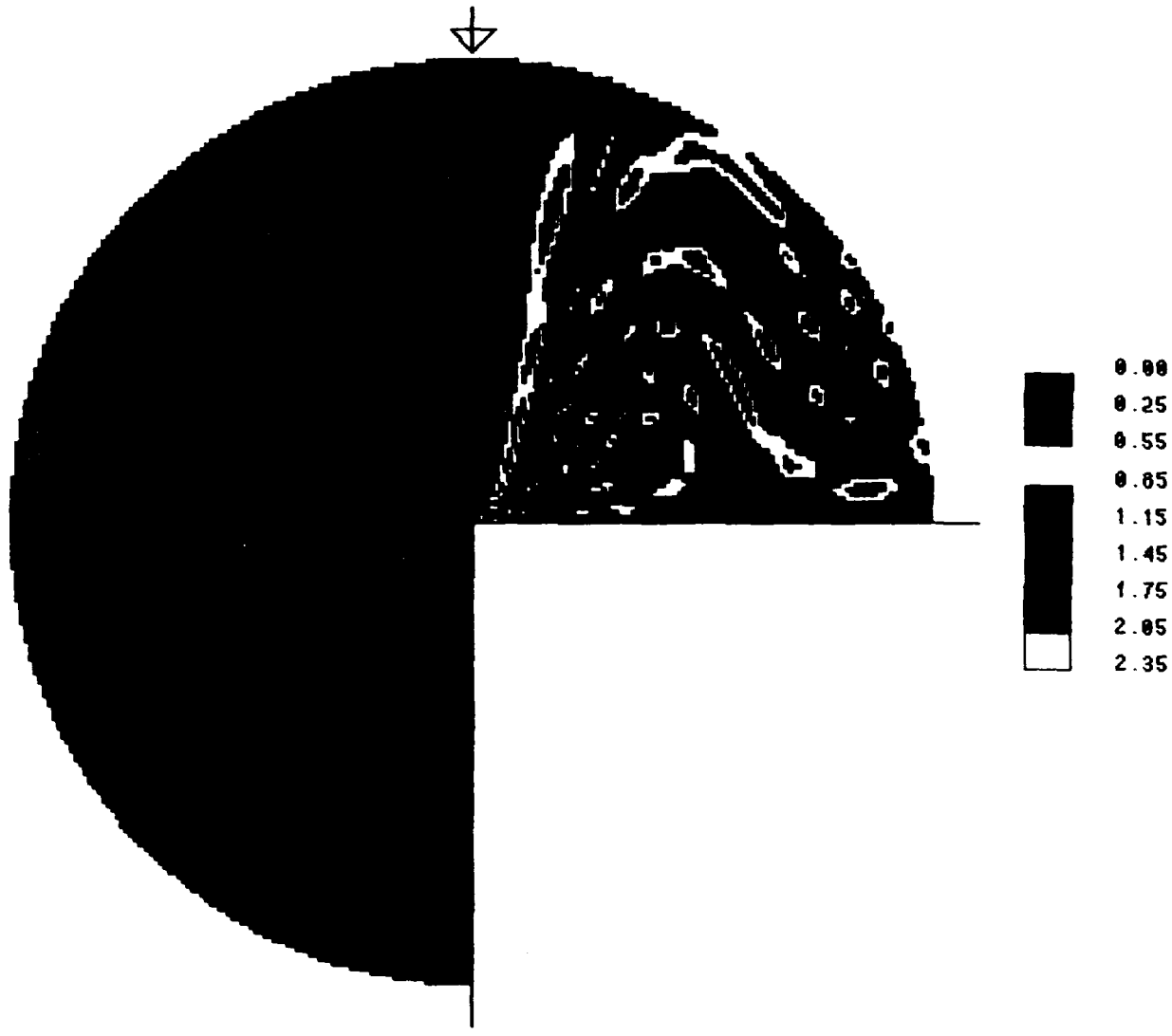


Figure 24. Amplification factor diagram for the 90-deg wedge for incident wave angle = 90 deg

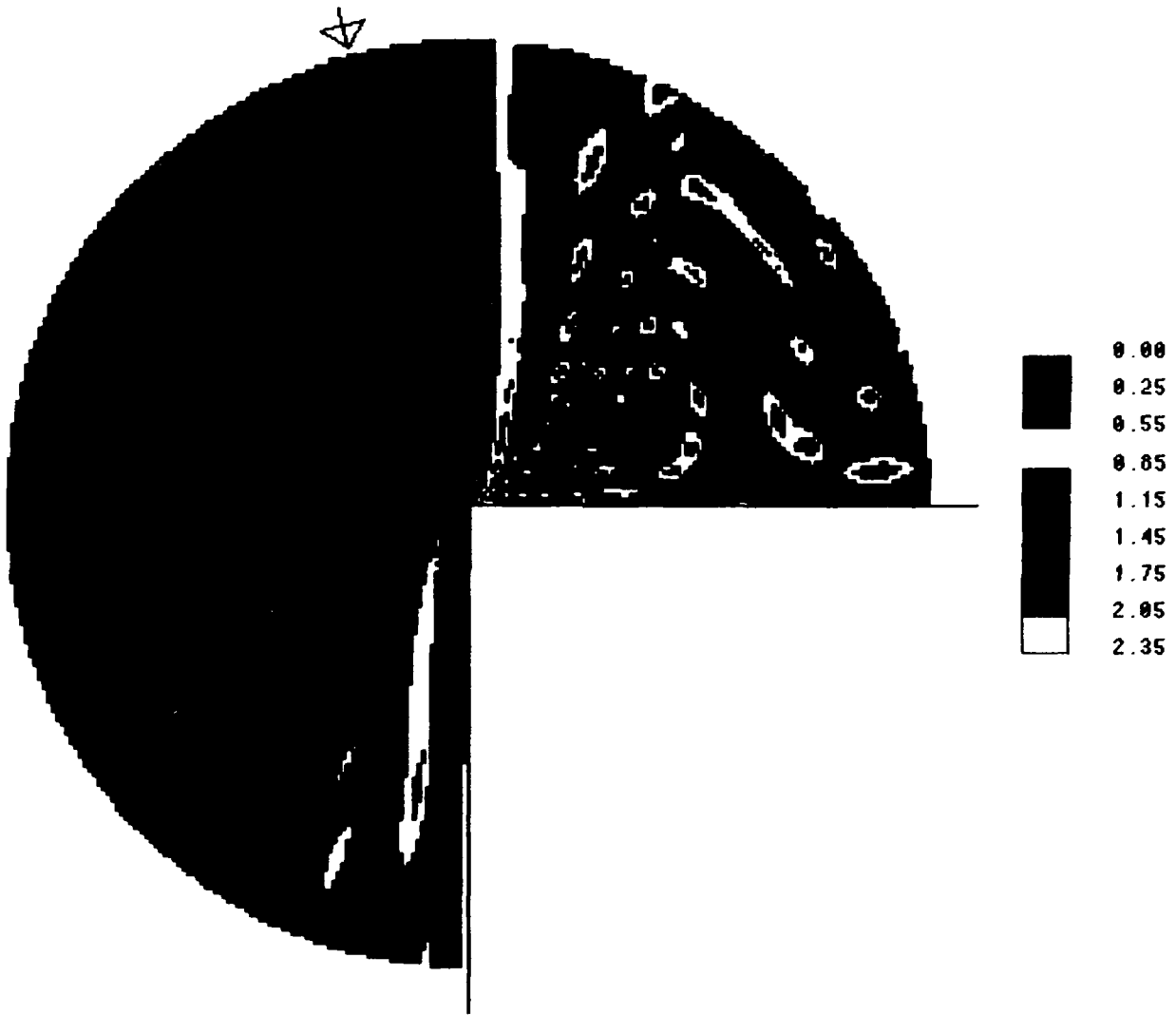


Figure 25. Amplification factor diagram for the 90-deg wedge for incident wave angle = 105 deg

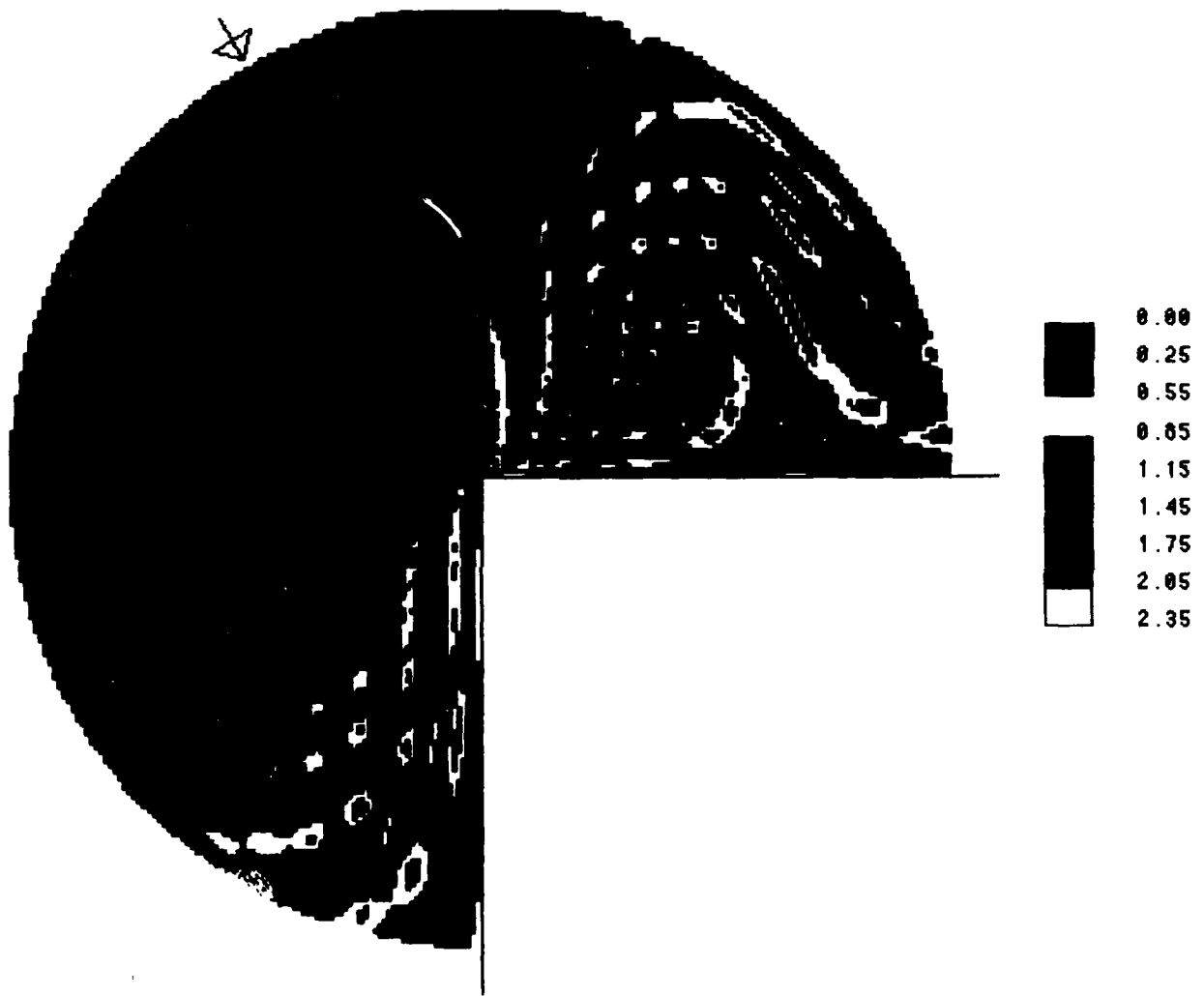


Figure 26. Amplification factor diagram for the 90-deg wedge for incident wave angle = 120 deg

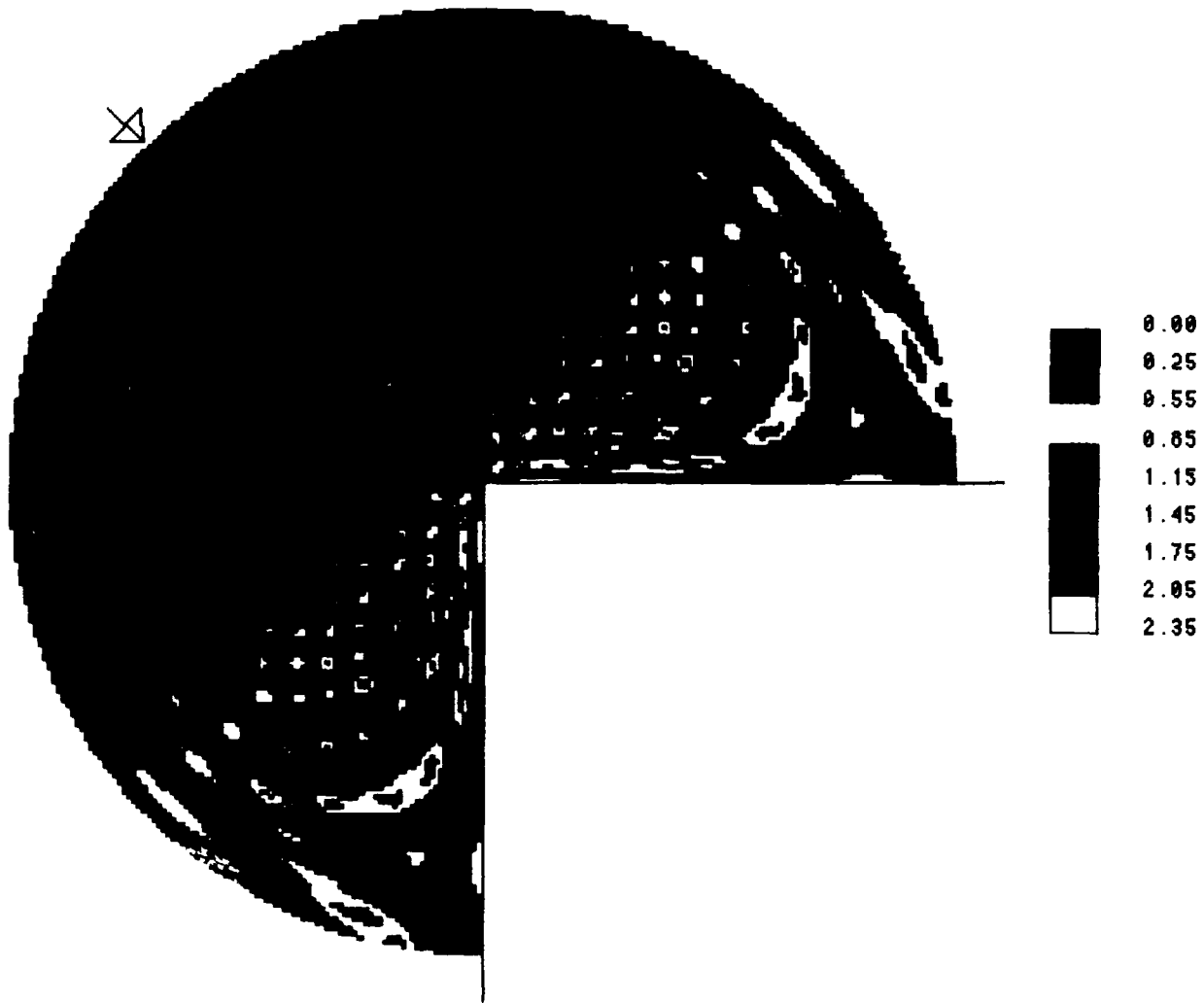


Figure 27. Amplification factor diagram for the 90-deg wedge for incident wave angle = 135 deg

#### PART IV: CONCLUSION

32. An analytical solution for the combined wave reflection and diffraction by a vertical wedge of arbitrary wedge angle is obtained and expressed in Equation 26. The analytical solution is in terms of Bessel functions and in nonclosed form. The computer subroutine WEDGE, written for calculating the solution, is documented in Appendix A.

33. The amplification factor diagrams for a vertical wedge of 0-deg wedge angle and a vertical wedge of 90-deg wedge angle are calculated and presented. The calculated results indicate that the wave response in subregion I, where the incident, reflected, and scattered waves all exist, is in a very complex pattern with the amplification factor varying from 2.35 to 0.0 over the subregion. The wave response in subregions II and III is a relatively simple pattern with the amplification factor decreasing from 1.15 roughly along the reflected wave ray reflected from the origin point to nearly 0.00 at the back wall of the wedge in the shadow zone.

34. Diagrams of the special case of a vertical wedge of 0-deg wedge angle can be considered complementary and extended versions to the ones presented in the SPM (1984).

## REFERENCES

Abramowitz, M., and Stegun, I. A. 1964 (Jun). Handbook of Mathematical Functions, National Bureau of Standards, Applied Mathematics Series 55, pp 358-495.

Morris, A. H., Jr. 1984 (Jun). "NSWC Library of Mathematics Subroutines," NSWC TR 84-143, Strategic Systems Department, Naval Surface Weapons Center, Dahlgren, Va., pp 43-44.

Shore Protection Manual. 1984. 4th ed., 2 vols, US Army Engineer Waterways Experiment Station, Coastal Engineering Research Center, US Government Printing Office, Washington, DC.

Stoker, J. J. 1957. Water Waves, Interscience Publishers, Inc., New York, pp 109-133.

Wiegel, R. L. 1962. (Jan). "Diffraction of Waves by a Semi-infinite Breaker," Journal of the Hydraulics Division, American Society of Civil Engineers, Vol 88, No. HY1, pp 27-44.

## APPENDIX A: SUBROUTINE WEDGE

1. Subroutine WEDGE is used to calculate the value of  $\phi$  in Equation 26 which is generally a complex number. Its absolute value is the amplification factor, and its phase is the phase indicator from the phase of the incident wave. As mentioned in the main text,  $\phi$  is a function of the Bessel function of either fractional or integer order, depending on the wedge angle, and is the summation of a series of infinite terms. The subroutine BESJ, documented in the Naval Surface Weapons Center (NSWC) Library of Mathematics Subroutines (Morris 1984)\* is used in the WEDGE subroutine. The programming of the WEDGE subroutine is very straightforward if a truncation term in the series in Equation 26 is determined. The program is written in FORTRAN language and is listed in this appendix.

### Description

2. The following subroutine is available for computing  $\phi$  in Equation 26:

```
CALL WEDGE(F, FABS, FPHA, XRL, XTH, WEDGEA, WAVEA, IDX)
```

where the arguments are all real values except F which is a complex value.

Input arguments are as follows:

- a. (XRL, XTH) =  $(r/\lambda, \theta)$  where  $(r, \theta)$  are polar coordinates of the location where  $\phi$  is to be computed, and  $\lambda$  is the incident wave length. Therefore, XRL is the radius vector or radius distance normalized by the incident wave length. XTH is the vectorial angle in degree.
- b. WEDGEA = wedge angle in degree.
- c. WAVEA = incident wave angle in degree.
- d. IDX = an index (set to 0 in this subroutine).

Output arguments are as follows:

---

\* References cited in the Appendix can be found in the References at the end of the main text.

- a.  $F = \phi$  in Equation 26 (wave response normalized by incident wave amplitude).
- b. FABS = amplification factor, the absolute value of  $\phi$ .
- c. FPHA = phase difference, the phase of  $\phi$ .

Example and Test Run

3. To serve as an example as well as to ensure the subroutine is the correct one, the user should run the test program listed in Figure A1 and make sure the output is the same as that listed in Table A1.

```

PROGRAM WEDGE1(INPUT,OUTPUT,TAPE5=INPUT,TAPE6=OUTPUT)
COMPLEX F
PI=3.141592654
WRITE(6,4)
4 FORMAT(/3X,' WEDG-ANG WAV-ANG      LOCATION      WAVE RESPONSE TEST5
1 ABS-VAL  PHASE' /3X,' (DEG)      (DEG)      XRL  XTH(DEG)      (NORMTEST6
2ALIZED)  AMP-FAC  (RAD)' /3X,35(' -')//)
WEDGEA=90.
WAVEA=135.
XRL=2.0
XTH=30.
IDX=0
CALL WEDGE(F,FABS,FPHA,XRL,XTH,WEDGEA,WAVEA,IDX)
WRITE(6,40) WEDGEA,WAVEA,XRL,XTH,F,FABS,FPHA
40 FORMAT(1X,BF9.2)
STOP
END
TEST1
TEST2
TEST3
TEST4
TEST5
TEST6
TEST7
TEST8
TEST9
TEST10
TEST11
TEST12
TEST13
TEST14
TEST15
TEST16
TEST17

```

Figure A1. Computer program list 1

Table A1  
Sample Output of the Test Program

WEDG-ANG (DEG)	WAV-ANG (DEG)	LOCATION XRL XTH(DEG)		WAVE RESPONSE (NORMALIZED)	ABS-VAL AMP-FAC	PHASE (RAD)
90.00	135.00	2.00	30.00	-.41	.68	.79
						2.11

4. The input arguments in the test programs are as follows:
  - a. WEDGEA = 90; the wedge angle is 90 deg.
  - b. WAVEA = 135; the incident wave angle is 135 deg.
  - c. XRL = 2.0 and XTH = 30; the location of the wave response  $\phi$  to be computed is at radial vector of two incident wave length distances and vectorial angle of 30 deg in polar coordinates.
  - d. IDX = 0; the index IDX is set to 0.

This case is shown in Figure A2. The outputs are given in Table A1 which is self-explanatory.

5. If the location of the wave response  $\phi$  to be computed is a very large distance, for example XRL greater than 18 or so, the output might print the message that the number of terms is insufficient for summation in computing  $\phi$ . In this situation, the user must replace the integer 200 in PARAMETER(NN=200), listed in Card WEDGE15 in the SUBROUTINE WEDGE list, by a larger integer to ensure the accuracy.

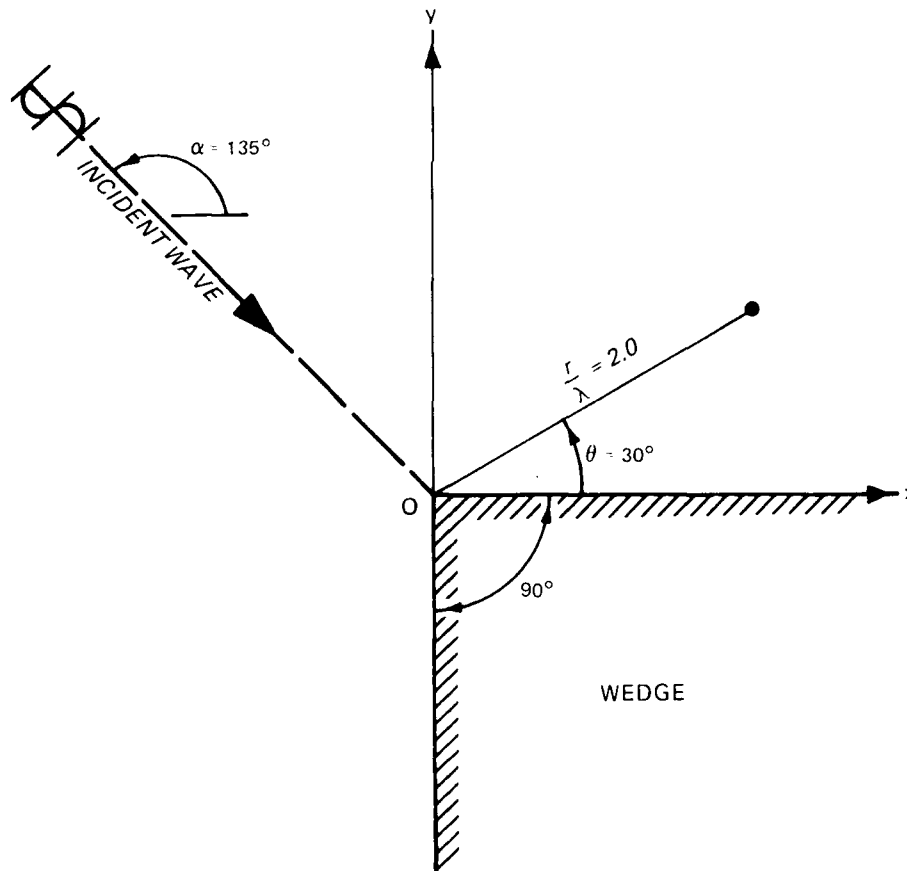


Figure A2. Example problem

### Subroutine WEDGE Listing

6. Subroutine WEDGE, which is listed in this section, calls subroutine BESJ which, in turn, calls subroutine JAIRY and function GAMLN. Subroutines BESJ and JAIRY and function GAMLN are borrowed from the NSWC Library of Mathematics Subroutines (Morris 1984). Including these borrowed subroutines here in the list is only for the purpose of allowing subroutine WEDGE to be self-contained and complete. The computer program of subroutine WEDGE is listed in Figure A3.



```

      IF (ABS(BJ(N1)).GT.TOLR) ICOUNT=0
10  CONTINUE
14  CONTINUE
      F=BJ(1)/2.
      DO 20 N=1,NNN
      N1=N+1
      XMN=XM(N1)
      TM=(0.0,1.0)**XMN*BJ(N1)*COS(XMN*WA)*COS(XMN*TH)
      F=F+TM
20  CONTINUE
      F=4./XNU*F
      FR=REAL(F)
      FI=AIMAG(F)
      FABS=SQRT(FR*FR+FI*FI)
      IF(WA.LE.1.E-8) FABS=FABS/2.
      IF(FABS.LT.TOLR) GOTO 30
      FPHA=ATAN2(FI,FR)
      RETURN
30  FPHA=0.0
      RETURN
      END
      SUBROUTINE BESJ(X,ALPHA,N,Y,NZ)
C  -----
C  WRITTEN BY D.E. AMOS, S.L. DANIEL AND M.K. WESTON, JANUARY, 1975.
C  REFERENCE SAND-75-0147
C
C  ABSTRACT
C  BESJ COMPUTES AN N MEMBER SEQUENCE OF J BESSEL FUNCTIONS
C  J/SUB(ALPHA+K-1)/(X), K=1,...,N FOR NON-NEGATIVE ALPHA AND X.
C  A COMBINATION OF THE POWER SERIES, THE ASYMPTOTIC EXPANSION
C  FOR X TO INFINITY AND THE UNIFORM ASYMPTOTIC EXPANSION FOR
C  NU TO INFINITY ARE APPLIED OVER SUBDIVISIONS OF THE (NU,X)
C  PLANE. FOR VALUES OF (NU,X) NOT COVERED BY ONE OF THESE
C  FORMULAE, THE ORDER IS INCREMENTED OR DECREMENTED BY INTEGER
C  VALUES INTO A REGION WHERE ONE OF THE FORMULAE APPLY. BACKWARD
C  RECURSION IS APPLIED TO REDUCE ORDERS BY INTEGER VALUES EXCEPT
C  WHERE THE ENTIRE SEQUENCE LIES IN THE OSCILLATORY REGION. IN
C  THIS CASE FORWARD RECURSION IS STABLE AND VALUES FROM THE
C  ASYMPTOTIC EXPANSION FOR X TO INFINITY START THE RECURSION
C  WHEN IT IS EFFICIENT TO DO SO. LEADING TERMS OF THE SERIES AND
C  UNIFORM EXPANSION ARE TESTED FOR UNDERFLOW. IF A SEQUENCE IS
C  REQUESTED AND THE LAST MEMBER WOULD UNDERFLOW, THE RESULT IS
C  SET TO ZERO AND THE NEXT LOWER ORDER TRIED, ETC., UNTIL A
C  MEMBER COMES ON SCALE OR ALL MEMBERS ARE SET TO ZERO. OVERFLOW
C  CANNOT OCCUR. BESJ1 CALLS SUBROUTINE JAIKY AND FUNCTION GAMLN.
C
C  DESCRIPTION OF ARGUMENTS
C
C  INPUT
C  X          - X.GE.0
C  ALPHA     - ORDER OF FIRST MEMBER OF THE SEQUENCE, ALPHA.GE.0
C  N         - NUMBER OF MEMBERS IN THE SEQUENCE, N.GE.1
C  OUTPUT
C  Y         - A VECTOR WHOSE FIRST N COMPONENTS CONTAIN
C              VALUES FOR J/SUB(ALPHA+K-1)/(X), K=1,...,N

```

Figure A3. (Sheet 2 of 25)

C	NZ	- ERROR INDICATOR	BESJ135
C		NZ=0 NORMAL RETURN - COMPUTATION COMPLETED	BESJ136
C		NZ=-1 X IS LESS THAN 0.0	BESJ137
C		NZ=-2 ALPHA IS LESS THAN 0.0	BESJ138
C		NZ=-3 N IS LESS THAN 1	BESJ139
C		NZ.GT.0 LAST NZ COMPONENTS OF Y SET TO 0.0	BESJ140
C		BECAUSE OF UNDERFLOW	BESJ141
C			BESJ142
C	ERROR CONDITIONS		BESJ143
C			BESJ144
C	IMPROPER INPUT ARGUMENTS - A FATAL ERROR		BESJ145
C	UNDERFLOW - A NON-FATAL ERROR (NZ.GT.0)		BESJ146
C			BESJ147
C	-----		BESJ148
C			BESJ149
	DOUBLE PRECISION DX,TRX,DTM,DFN		BESJ150
	DIMENSION Y(N)		BESJ151
	DIMENSION C(11,10),ALFA(26,4),BETA(26,5)		BESJ152
	DIMENSION C1(88),C2(22)		BESJ153
	DIMENSION A1(52),A2(52),B1(52),B2(52),B3(26)		BESJ154
	DIMENSION GAMA(26),TEMP(3),KMAX(5),AR(8),BR(10),UPOL(10)		BESJ155
	DIMENSION FNULIM(2),PP(4)		BESJ156
	DIMENSION CR(10),DR(10)		BESJ157
C			BESJ158
	EQUIVALENCE (C(1,1),C1(1))		BESJ159
	EQUIVALENCE (C(1,9),C2(1))		BESJ160
	EQUIVALENCE (ALFA(1,1),A1(1))		BESJ161
	EQUIVALENCE (ALFA(1,3),A2(1))		BESJ162
	EQUIVALENCE (BETA(1,1),B1(1))		BESJ163
	EQUIVALENCE (BETA(1,3),B2(1))		BESJ164
	EQUIVALENCE (BETA(1,5),B3(1))		BESJ165
C			BESJ166
	DATA ELIM1,ELIM2,TOL / 667. , 644. , 1.E-15		/BESJ167
C			BESJ168
	DATA PP(1)/8.7290915393555E+00/, PP(2)/2.6569373226503E-01/,		BESJ169
1	PP(3)/1.2457857686559E-01/, PP(4)/7.7013374743039E-04/		BESJ170
C			BESJ171
	TOLS=LN(1.E-3)		BESJ172
C	DATA TOLS /-6.9077552789821E+00/		BESJ173
C			BESJ174
	DATA UPOL(1),CON1,CON2,CON3,CON548 / 1.0000000000000E+00,		BESJ175
1	6.6666666666667E-01, 3.3333333333333E-01, 1.4142135623731E+00,		BESJ176
2	1.0416666666667E-01/		BESJ177
C			BESJ178
	DATA RTWO,PDF,RTTP,PIDT / 1.3483997249265E+00,		BESJ179
1	7.8539816339745E-01, 7.9788456080286E-01, 1.5707963267949E+00/		BESJ180
C			BESJ181
	DATA FNULIM(1)/100./, FNULIM(2)/60./		BESJ182
C			BESJ183
	CE=-ALOG(TOL) , TCE=-0.75*ALOG(TOL)		BESJ184
C	DATA CE , TCE / 3.4538776394911E+01, 2.5904082296183E+01/		BESJ185
C			BESJ186
	DATA INLIM / 150 /		BESJ187
C			BESJ188
	DATA AR(1)/8.3550347222222E-02/, AR(2)/1.2822657455633E-01/,		BESJ189A

Figure A3. (Sheet 3 of 25)

	1	AR(3)/2.9184902646414E-01/,	AR(4)/8.8162726744376E-01/,	BESJ189B		
	2	AR(5)/3.3214082818628E+00/,	AR(6)/1.4995762986863E+01/,	BESJ189C		
	3	AR(7)/7.8923013011586E+01/,	AR(8)/4.7445153886826E+02/	BESJ189D		
C				BESJ190		
		DATA BR(1) /-1.4583333333333E-01/,	BR(2) /-9.8741319444444E-02/,	BSEJ191A		
	1	BR(3) /-1.4331205391590E-01/,	BR(4) /-3.1722720267841E-01/,	BSEJ191B		
	2	BR(5) /-9.4242914795712E-01/,	BR(6) /-3.5112030408264E+00/,	BSEJ191C		
	3	BR(7) /-1.5727263620368E+01/,	BR(8) /-8.2281439097186E+01/,	BSEJ191D		
	4	BR(9) /-4.9235537052367E+02/,	BR(10)/-3.3162185685480E+03/	BSEJ191E		
C				BESJ192		
		DATA C1(1) /-2.0833333333333E-01/,	C1(2) / 1.2500000000000E-01/,	BESJ193A		
	1	C1(3) / 0.0/,	C1(4) / 0.0/,	C1(5) / 0.0/,	C1(6) / 0.0/,	BESJ193B
	2	C1(7) / 0.0/,	C1(8) / 0.0/,	C1(9) / 0.0/,	C1(10)/ 0.0/,	BESJ193C
	3	C1(11)/ 0.0/,	C1(12)/ 3.3420138888889E-01/,			BESJ193D
	4	C1(13)/-4.0104166666667E-01/,	C1(14)/ 7.0312500000000E-02/,			BESJ193E
	5	C1(15)/ 0.0/,	C1(16)/ 0.0/,	C1(17)/ 0.0/,	C1(18)/ 0.0/,	BESJ193F
	6	C1(19)/ 0.0/,	C1(20)/ 0.0/,	C1(21)/ 0.0/,	C1(22)/ 0.0/,	BESJ193G
	7	C1(23)/-1.0258125964506E+00/,	C1(24)/ 1.8464626736111E+00/,			BESJ193H
	8	C1(25)/-8.9121093750000E-01/,	C1(26)/ 7.3242187500000E-02/,			BESJ193I
	9	C1(27)/ 0.0/,	C1(28)/ 0.0/,	C1(29)/ 0.0/,	C1(30)/ 0.0/,	BESJ193J
	1	C1(31)/ 0.0/,	C1(32)/ 0.0/,	C1(33)/ 0.0/,		BESJ193K
	2	C1(34)/ 4.6695844234262E+00/,	C1(35)/-1.1207002616223E+01/,			BESJ193L
	3	C1(36)/ 8.7891235351562E+00/,	C1(37)/-2.3640869140625E+00/,			BESJ193M
	4	C1(38)/ 1.1215209960938E-01/,	C1(39)/ 0.0/,	C1(40)/ 0.0/,		BESJ193N
	5	C1(41)/ 0.0/,	C1(42)/ 0.0/,	C1(43)/ 0.0/,	C1(44)/ 0.0/,	BESJ193O
	6	C1(45)/-2.8212072558200E+01/,	C1(46)/ 8.4636217674601E+01/,			BESJ193P
	7	C1(47)/-9.1818241543240E+01/,	C1(48)/ 4.2534998745388E+01/,			BESJ193Q
	8	C1(49)/-7.3687943594796E+00/,	C1(50)/ 2.2710800170898E-01/,			BESJ193R
	9	C1(51)/ 0.0/,	C1(52)/ 0.0/,	C1(53)/ 0.0/,	C1(54)/ 0.0/	BESJ193S
C						BESJ194
		DATA C1(55)/ 0.0/,	C1(56)/ 2.1257013003922E+02/,			BESJ195A
	1	C1(57)/-7.6525246814118E+02/,	C1(58)/ 1.0599904525280E+03/,			BESJ195B
	2	C1(59)/-6.9957962737613E+02/,	C1(60)/ 2.1819051174421E+02/,			BESJ195C
	3	C1(61)/-2.6491430486952E+01/,	C1(62)/ 5.7250142097473E-01/,			BESJ195D
	4	C1(63)/ 0.0/,	C1(64)/ 0.0/,	C1(65)/ 0.0/,	C1(66)/ 0.0/,	BESJ195E
	5	C1(67)/-1.9194576623184E+03/,	C1(68)/ 8.0617221817373E+03/,			BESJ195F
	6	C1(69)/-1.3586550006434E+04/,	C1(70)/ 1.1655393336864E+04/,			BESJ195G
	7	C1(71)/-5.3056469786134E+03/,	C1(72)/ 1.2009029132164E+03/,			BESJ195H
	8	C1(73)/-1.0809091978840E+02/,	C1(74)/ 1.7277275025845E+00/,			BESJ195I
	9	C1(75)/ 0.0/,	C1(76)/ 0.0/,	C1(77)/ 0.0/,		BESJ195J
	1	C1(78)/ 2.0204291330966E+04/,	C1(79)/-9.6980598388638E+04/,			BESJ195K
	2	C1(80)/ 1.9254700123253E+05/,	C1(81)/-2.0340017728042E+05/,			BESJ195L
	3	C1(82)/ 1.2220046498302E+05/,	C1(83)/-4.1192654968898E+04/,			BESJ195M
	4	C1(84)/ 7.1095143024894E+03/,	C1(85)/-4.9391530477309E+02/,			BESJ195N
	5	C1(86)/ 6.0740420012735E+00/,	C1(87)/ 0.0/,	C1(88)/ 0.0/		BESJ195O
C						BESJ196
		DATA C2(1) /-2.4291918790055E+05/,	C2(2) / 1.3117636146630E+06/,			BESJ197A
	1	C2(3) /-2.9980159185381E+06/,	C2(4) / 3.7632712976564E+06/,			BESJ197B
	2	C2(5) /-2.8135632265865E+06/,	C2(6) / 1.2683652733216E+06/,			BESJ197C
	3	C2(7) /-3.3164517248456E+05/,	C2(8) / 4.5218768981363E+04/,			BESJ197D
	4	C2(9) /-2.4998304818112E+03/,	C2(10)/ 2.4380529699556E+01/,			BESJ197E
	5	C2(11)/ 0.0/,	C2(12)/ 3.2844698530720E+06/,			BESJ197F
	6	C2(13)/-1.9706819118432E+07/,	C2(14)/ 5.0952602492665E+07/,			BESJ197G
	7	C2(15)/-7.4105148211533E+07/,	C2(16)/ 6.6344512274729E+07/,			BESJ197H
	8	C2(17)/-3.7567176660763E+07/,	C2(18)/ 1.3288767166422E+07/,			BESJ197I

Figure A3. (Sheet 4 of 25)

9	C2(19) / -2.7856181280864E+06 /,	C2(20) / 3.0818640461266E+05 /,	BESJ197J
1	C2(21) / -1.3886089753717E+04 /,	C2(22) / 1.1001714026925E+02 /	BESJ197K
			BESJ198
	DATA A1(1) / -4.4444444444444E-03 /,	A1(2) / -9.2207772207792E-04 /,	BESJ199A
1	A1(3) / -8.8489288489288E-05 /,	A1(4) / 1.6592768783245E-04 /,	BESJ199B
2	A1(5) / 2.4669137274179E-04 /,	A1(6) / 2.6599558934626E-04 /,	BESJ199C
3	A1(7) / 2.6182429706150E-04 /,	A1(8) / 2.4873043734466E-04 /,	BESJ199D
4	A1(9) / 2.3272104008323E-04 /,	A1(10) / 2.1636248571236E-04 /,	BESJ199E
5	A1(11) / 2.0073885876275E-04 /,	A1(12) / 1.8626763663754E-04 /,	BESJ199F
6	A1(13) / 1.7306077591788E-04 /,	A1(14) / 1.6109170592902E-04 /,	BESJ199G
7	A1(15) / 1.5027477416091E-04 /,	A1(16) / 1.4050349739127E-04 /,	BESJ199H
8	A1(17) / 1.3166881654592E-04 /,	A1(18) / 1.2366744559825E-04 /,	BESJ199I
9	A1(19) / 1.1640527147474E-04 /,	A1(20) / 1.0979829837271E-04 /,	BESJ199J
1	A1(21) / 1.0377241042299E-04 /,	A1(22) / 9.8262607836936E-05 /,	BESJ199K
2	A1(23) / 9.3212051724950E-05 /,	A1(24) / 8.8571085247871E-05 /,	BESJ199L
3	A1(25) / 8.4296310571570E-05 /,	A1(26) / 8.0349754840779E-05 /,	BESJ199M
4	A1(27) / 6.9373554135459E-04 /,	A1(28) / 2.3224174518292E-04 /,	BESJ199N
5	A1(29) / -1.4198627355669E-05 /,	A1(30) / -1.1644493167205E-04 /,	BESJ199O
6	A1(31) / -1.5080355805305E-04 /,	A1(32) / -1.5512192491810E-04 /,	BESJ199P
7	A1(33) / -1.4680975664647E-04 /,	A1(34) / -1.3381550386749E-04 /,	BESJ199Q
8	A1(35) / -1.1974497568425E-04 /,	A1(36) / -1.0618431920797E-04 /,	BESJ199R
9	A1(37) / -9.3769954989119E-05 /,	A1(38) / -8.2692304558819E-05 /	BESJ199S
			BESJ200
	DATA A1(39) / -7.2937434815522E-05 /,	A1(40) / -6.4404235772102E-05 /,	BESJ201A
1	A1(41) / -5.6961156600937E-05 /,	A1(42) / -5.0473104430356E-05 /,	BESJ201B
2	A1(43) / -4.4813486800888E-05 /,	A1(44) / -3.9868872771760E-05 /,	BESJ201C
3	A1(45) / -3.5540053297204E-05 /,	A1(46) / -3.1741425660902E-05 /,	BESJ201D
4	A1(47) / -2.8399679390418E-05 /,	A1(48) / -2.5452272063487E-05 /,	BESJ201E
5	A1(49) / -2.2845929716472E-05 /,	A1(50) / -2.0535275310648E-05 /,	BESJ201F
6	A1(51) / -1.8481621762767E-05 /,	A1(52) / -1.6651933002139E-05 /	BESJ201G
			BESJ202
	DATA A2(1) / -3.5421197145774E-04 /,	A2(2) / -1.5616126394516E-04 /,	BESJ203A
1	A2(3) / 3.0446550359494E-05 /,	A2(4) / 1.3019865577324E-04 /,	BESJ203B
2	A2(5) / 1.6747110669971E-04 /,	A2(6) / 1.7022258768359E-04 /,	BESJ203C
3	A2(7) / 1.5650142760860E-04 /,	A2(8) / 1.3633917097744E-04 /,	BESJ203D
4	A2(9) / 1.1488669202982E-04 /,	A2(10) / 9.4586909303469E-05 /,	BESJ203E
5	A2(11) / 7.6449841925090E-05 /,	A2(12) / 6.0757033496520E-05 /,	BESJ203F
6	A2(13) / 4.7439429929051E-05 /,	A2(14) / 3.6275751200534E-05 /,	BESJ203G
7	A2(15) / 2.6993971497922E-05 /,	A2(16) / 1.9321093824794E-05 /,	BESJ203H
8	A2(17) / 1.3005667479396E-05 /,	A2(18) / 7.8262086674450E-06 /,	BESJ203I
9	A2(19) / 3.5925748581935E-06 /,	A2(20) / 1.4404004981425E-07 /,	BESJ203J
1	A2(21) / -2.6539676969794E-06 /,	A2(22) / -4.9134686709849E-06 /,	BESJ203K
2	A2(23) / -6.7273929609125E-06 /,	A2(24) / -8.1726937967866E-06 /,	BESJ203L
3	A2(25) / -9.3130471509356E-06 /,	A2(26) / -1.0201141879802E-05 /,	BESJ203M
4	A2(27) / 3.7819419920177E-04 /,	A2(28) / 2.0247195276182E-04 /,	BESJ203N
5	A2(29) / -6.3793850631886E-05 /,	A2(30) / -2.3859823060301E-04 /,	BESJ203O
6	A2(31) / -3.1091625602736E-04 /,	A2(32) / -3.1368011524758E-04 /,	BESJ203P
7	A2(33) / -2.7895027379132E-04 /,	A2(34) / -2.2856408261914E-04 /,	BESJ203Q
8	A2(35) / -1.7524528034085E-04 /,	A2(36) / -1.2554406306069E-04 /,	BESJ203R
9	A2(37) / -8.2298287282021E-05 /,	A2(38) / -4.6286073058812E-05 /	BESJ203S
			BESJ204
	DATA A2(39) / -1.7233430236696E-05 /,	A2(40) / 5.6069048230460E-06 /,	BESJ205A
1	A2(41) / 2.3139544314829E-05 /,	A2(42) / 3.6264274585679E-05 /,	BESJ205B
2	A2(43) / 4.5800612449019E-05 /,	A2(44) / 5.2459529495911E-05 /,	BESJ205C
3	A2(45) / 5.6839620854582E-05 /,	A2(46) / 5.9434982039310E-05 /,	BESJ205D

Figure A3. (Sheet 5 of 25)

	4	A2(47) / 6.0647852757842E-05 /	A2(48) / 6.0802390778844E-05 /	BESJ205E
	5	A2(49) / 6.0157789453946E-05 /	A2(50) / 5.8919965734470E-05 /	BESJ205F
	6	A2(51) / 5.7251582377759E-05 /	A2(52) / 5.5280437558585E-05 /	BESJ205G
C				BESJ20
		DATA B1(1) / 1.7998872141355E-02 /	B1(2) / 5.5996491106439E-03 /	BESJ207A
	1	B1(3) / 2.8850140223113E-03 /	B1(4) / 1.8009660676105E-03 /	BESJ207B
	2	B1(5) / 1.2475311058920E-03 /	B1(6) / 9.2287887657294E-04 /	BESJ207C
	3	B1(7) / 7.1443042172729E-04 /	B1(8) / 5.7178728178970E-04 /	BESJ207D
	4	B1(9) / 4.6943100760648E-04 /	B1(10) / 3.9323283546292E-04 /	BESJ207E
	5	B1(11) / 3.3481888931830E-04 /	B1(12) / 2.8895214849575E-04 /	BESJ207F
	6	B1(13) / 2.5221161554957E-04 /	B1(14) / 2.2228058079888E-04 /	BESJ207G
	7	B1(15) / 1.9754183803306E-04 /	B1(16) / 1.7683685501972E-04 /	BESJ207H
	8	B1(17) / 1.5931689966182E-04 /	B1(18) / 1.4434793019733E-04 /	BESJ207I
	9	B1(19) / 1.3144806811996E-04 /	B1(20) / 1.2024544494930E-04 /	BESJ207J
	1	B1(21) / 1.1044914450460E-04 /	B1(22) / 1.0182877074057E-04 /	BESJ207K
	2	B1(23) / 9.4199822420424E-05 /	B1(24) / 8.7413054575383E-05 /	BESJ207L
	3	B1(25) / 8.1346626216280E-05 /	B1(26) / 7.5900226964622E-05 /	BESJ207M
	4	B1(27) / -1.4928295321343E-03 /	B1(28) / -8.7820470954639E-04 /	BESJ207N
	5	B1(29) / -5.0291654957204E-04 /	B1(30) / -2.9482213851275E-04 /	BESJ207O
	6	B1(31) / -1.7546399697078E-04 /	B1(32) / -1.0400855046082E-04 /	BESJ207P
	7	B1(33) / -5.9614195304646E-05 /	B1(34) / -3.1203892907610E-05 /	BESJ207Q
	8	B1(35) / -1.2608973598023E-05 /	B1(36) / -2.4289260857573E-07 /	BESJ207R
	9	B1(37) / 8.0599616541427E-06 /	B1(38) / 1.3650700926215E-05 /	BESJ207S
C				BESJ208
		DATA B1(39) / 1.7396412547293E-05 /	B1(40) / 1.9867297884213E-05 /	BESJ209A
	1	B1(41) / 2.1446326379082E-05 /	B1(42) / 2.2395465923246E-05 /	BESJ209B
	2	B1(43) / 2.2896778381471E-05 /	B1(44) / 2.3078538981118E-05 /	BESJ209C
	3	B1(45) / 2.3032197608091E-05 /	B1(46) / 2.2823607372035E-05 /	BESJ209D
	4	B1(47) / 2.2500588110529E-05 /	B1(48) / 2.2098101536199E-05 /	BESJ209E
	5	B1(49) / 2.1641842744810E-05 /	B1(50) / 2.1150764925622E-05 /	BESJ209F
	6	B1(51) / 2.0638874978217E-05 /	B1(52) / 2.0116524199708E-05 /	BESJ209G
C				BESJ210
		DATA B2(1) / 5.5221307672129E-04 /	B2(2) / 4.4793258155238E-04 /	BESJ211A
	1	B2(3) / 2.7952065399202E-04 /	B2(4) / 1.5246815619845E-04 /	BESJ211B
	2	B2(5) / 6.9327110565704E-05 /	B2(6) / 1.7625868306999E-05 /	BESJ211C
	3	B2(7) / -1.3574499634327E-05 /	B2(8) / -3.1797241335043E-05 /	BESJ211D
	4	B2(9) / -4.1886186169669E-05 /	B2(10) / -4.6900488937914E-05 /	BESJ211E
	5	B2(11) / -4.8766544741379E-05 /	B2(12) / -4.8701003118674E-05 /	BESJ211F
	6	B2(13) / -4.7475562089009E-05 /	B2(14) / -4.5581305813863E-05 /	BESJ211G
	7	B2(15) / -4.3330964451127E-05 /	B2(16) / -4.0923019315775E-05 /	BESJ211H
	8	B2(17) / -3.8482263860322E-05 /	B2(18) / -3.6085716753541E-05 /	BESJ211I
	9	B2(19) / -3.3779330612337E-05 /	B2(20) / -3.1588856077211E-05 /	BESJ211J
	1	B2(21) / -2.9526956175081E-05 /	B2(22) / -2.7597891482834E-05 /	BESJ211K
	2	B2(23) / -2.5800617466688E-05 /	B2(24) / -2.4130835676128E-05 /	BESJ211L
	3	B2(25) / -2.2582350951835E-05 /	B2(26) / -2.1147965676891E-05 /	BESJ211M
	4	B2(27) / -4.7461779655996E-04 /	B2(28) / -4.7786456714732E-04 /	BESJ211N
	5	B2(29) / -3.2039022806704E-04 /	B2(30) / -1.6110501611996E-04 /	BESJ211O
	6	B2(31) / -4.2577810128544E-05 /	B2(32) / 3.4457129429497E-05 /	BESJ211P
	7	B2(33) / 7.9709268407568E-05 /	B2(34) / 1.0313823670827E-04 /	BESJ211Q
	8	B2(35) / 1.1246677526220E-04 /	B2(36) / 1.1310364210848E-04 /	BESJ211R
	9	B2(37) / 1.0865163484877E-04 /	B2(38) / 1.0143795159766E-04 /	BESJ211S
C				BESJ212
		DATA B2(39) / 9.2929839659336E-05 /	B2(40) / 8.4029313301609E-05 /	BESJ213A
	1	B2(41) / 7.5272799134913E-05 /	B2(42) / 6.6963252197573E-05 /	BESJ213B
	2	B2(43) / 5.9256454732320E-05 /	B2(44) / 5.2216930882698E-05 /	BESJ213C

Figure A3. (Sheet 6 of 25)

	3	B2(45) / 4.5853948516536E-05 /,	B2(46) / 4.0144551389149E-05 /,	BESJ213D
	4	B2(47) / 3.5048173003133E-05 /,	B2(48) / 3.0515799503435E-05 /,	BESJ213E
	5	B2(49) / 2.4495611995052E-05 /,	B2(50) / 2.2936363369100E-05 /,	BESJ213F
	6	B2(51) / 1.9789305666402E-05 /,	B2(52) / 1.7009198463641E-05 /	BESJ213G
C				BESJ214
		DATA B3(1) / 7.3646581057258E-04 /,	B3(2) / 8.7279080514619E-04 /,	BESJ215A
	1	B3(3) / 6.2261486257314E-04 /,	B3(4) / 2.8599815419430E-04 /,	BESJ215B
	2	B3(5) / 3.8473767287937E-06 /,	B3(6) / -1.8790600363697E-04 /,	BESJ215C
	3	B3(7) / -2.9760364659456E-04 /,	B3(8) / -3.4599812683267E-04 /,	BESJ215D
	4	B3(9) / -3.5338247091604E-04 /,	B3(10) / -3.3571563577505E-04 /,	BESJ215E
	5	B3(11) / -3.0432112478904E-04 /,	B3(12) / -2.6672272304761E-04 /,	BESJ215F
	6	B3(13) / -2.2765421412282E-04 /,	B3(14) / -1.8992261185456E-04 /,	BESJ215G
	7	B3(15) / -1.5505891859909E-04 /,	B3(16) / -1.2377824076187E-04 /,	BESJ215H
	8	B3(17) / -9.6292614771764E-05 /,	B3(18) / -7.2517832771442E-05 /,	BESJ215I
	9	B3(19) / -5.2207002889563E-05 /,	B3(20) / -3.5034775051190E-05 /,	BESJ215J
	1	B3(21) / -2.0648976103555E-05 /,	B3(22) / -8.7010609684977E-06 /,	BESJ215K
	2	B3(23) / 1.1369868667510E-06 /,	B3(24) / 9.1642647412278E-06 /,	BESJ215L
	3	B3(25) / 1.5647778542887E-05 /,	B3(26) / 2.0822362948247E-05 /	BESJ215M
C				BESJ216
		DATA GAMA(1) / 6.2996052494744E-01 /,		BESJ217A
	1	GAMA(2) / 2.5198420997898E-01 /,	GAMA(3) / 1.5479030041566E-01 /,	BESJ217B
	2	GAMA(4) / 1.1071306241616E-01 /,	GAMA(5) / 8.5730939552740E-02 /,	BESJ217C
	3	GAMA(6) / 6.9716131695868E-02 /,	GAMA(7) / 5.8608567189371E-02 /,	BESJ217D
	4	GAMA(8) / 5.0469887353631E-02 /,	GAMA(9) / 4.4260058068916E-02 /,	BESJ217E
	5	GAMA(10) / 3.9372066154351E-02 /,	GAMA(11) / 3.5428319592446E-02 /,	BESJ217F
	6	GAMA(12) / 3.2181885750210E-02 /,	GAMA(13) / 2.9464624079116E-02 /,	BESJ217G
	7	GAMA(14) / 2.7158167711293E-02 /,	GAMA(15) / 2.5176827297386E-02 /,	BESJ217H
	8	GAMA(16) / 2.3457075530608E-02 /,	GAMA(17) / 2.1950839013491E-02 /,	BESJ217I
	9	GAMA(18) / 2.0621082823565E-02 /,	GAMA(19) / 1.9438824089788E-02 /,	BESJ217J
	1	GAMA(20) / 1.8381063380068E-02 /,	GAMA(21) / 1.7429321323196E-02 /,	BESJ217K
	2	GAMA(22) / 1.6568583778661E-02 /,	GAMA(23) / 1.5786528598792E-02 /,	BESJ217L
	3	GAMA(24) / 1.5072950149410E-02 /,	GAMA(25) / 1.4419325083996E-02 /,	BESJ217M
	4	GAMA(26) / 1.3818480573534E-02 /		BESJ217N
C		-----		BESJ218
C				BESJ219
C		TEST INPUT ARGUMENTS		BESJ220
C				BESJ221
		NZ=0		BESJ222
		KT=1		BESJ223
		IF(N-1) 92,108,109		BESJ224
	108	KT=2		BESJ225
	109	NN=N		BESJ226
		IF(X) 93,110,120		BESJ227
	110	IF(ALPHA) 91,114,116		BESJ228
	114	Y(1)=1.		BESJ229
		IF(N.EQ.1) RETURN		BESJ230
		I1=2		BESJ231
		GO TO 118		BESJ232
	116	I1=1		BESJ233
	118	DO 119 I=I1,N		BESJ234
	119	Y(I)=0.		BESJ235
		RETURN		BESJ236
	120	CONTINUE		BESJ237
		IF(ALPHA.LT.0.) GO TO 91		BESJ238
C				BESJ239

Figure A3. (Sheet 7 of 25)

	DFN=DBLE(FLOAT(N))+DBLE(ALPHA)-1.D+0	BESJ240
	FNU=DFN	BESJ241
	XQ2=X*.5	BESJ242
	SXQ2=XQ2*XQ2	BESJ243
C		BESJ244
C	DECISION TREE FOR REGION WHERE SERIES, ASYMPTOTIC EXPANSION FOR X	BESJ245
C	TO INFINITY AND ASYMPTOTIC EXPANSION FOR NU TO INFINITY ARE	BESJ246
C	APPLIED.	BESJ247
C		BESJ248
	IF(SXQ2.LE.(FNU+1.)) GO TO 850	BESJ249
	TA=AMAX1(20.,FNU)	BESJ250
	IF(X.GT.TA) GO TO 880	BESJ251
	IF(X.GT.12.) GO TO 860	BESJ252
	XQ2L=ALOG(XQ2)	BESJ253
	NS=SXQ2-FNU	BESJ254
	GO TO 852	BESJ255
850	FN=FNU	BESJ256
	FNP1=FN+1.	BESJ257
	XQ2L=ALOG(XQ2)	BESJ258
	IS=KT	BESJ259
	IF(X.LE.0.5) GO TO 134	BESJ260
	NS=0	BESJ261
852	DFN=DFN+DBLE(FLOAT(NS))	BESJ262
	FN=DFN	BESJ263
	FNP1=FN+1.	BESJ264
	IS=KT	BESJ265
	IF(N-1+NS.GT.0) IS=3	BESJ266
	GO TO 134	BESJ267
860	NS=AMAX1(36.-FNU,0.)	BESJ268
	DFN=DFN+DBLE(FLOAT(NS))	BESJ269
	FN=DFN	BESJ270
	IS=KT	BESJ271
	IF(N-1+NS.GT.0) IS=3	BESJ272
	GO TO 130	BESJ273
880	CONTINUE	BESJ274
	RTX=SQRT(X)	BESJ275
	TAU=RTWD*RTX	BESJ276
	TA=TAU+FNULIM(KT)	BESJ277
	IF(FNU.LE.TA) GO TO 500	BESJ278
129	FN=FNU	BESJ279
	IS=KT	BESJ280
C		BESJ281
C	UNIFORM ASYMPTOTIC EXPANSION FOR NU TO INFINITY	BESJ282
C		BESJ283
130	CONTINUE	BESJ284
	XX=X/FN	BESJ285
	W2=1.-XX*XX	BESJ286
	ABW2=ABS(W2)	BESJ287
	RA=SQRT(ABW2)	BESJ288
	IF(ABW2.GT.0.2775) GO TO 200	BESJ289
C		BESJ290
C	CASES NEAR X=FN, ABS(1.-(X/FN)**2).LE.0.2775	BESJ291
C	COEFFICIENTS OF ASYMPTOTIC EXPANSION BY SERIES	BESJ292
C		BESJ293
C		BESJ294

Figure A3. (Sheet 8 of 25)

C	ZETA AND TRUNCATION FOR A(ZETA) AND B(ZETA) SERIES	BESJ295
C		BESJ296
C	KMAX IS TRUNCATION INDEX FOR A(ZETA) AND B(ZETA) SERIES=MAX(2,SA)	BESJ297
C		BESJ298
	SA=0.	BESJ299
	IF(ABW2.EQ.0.) GO TO 21	BESJ300
	SA=TOLS/ALOG(ABW2)	BESJ301
21	SB=SA	BESJ302
	DO 22 I=1,5	BESJ303
	KMAX(I)=AMAX1(SA,2.)	BESJ304
	SA=SA+SB	BESJ305
22	CONTINUE	BESJ306
	KB=KMAX(5)	BESJ307
	KLAST=KB-1	BESJ308
	SA=GAMA(KB)	BESJ309
	DO 24 K=1,KLAST	BESJ310
	KB=KB-1	BESJ311
	SA=SA*W2+GAMA(KB)	BESJ312
24	CONTINUE	BESJ313
	Z=W2*SA	BESJ314
	AZ=ABS(Z)	BESJ315
	RTZ=SQRT(AZ)	BESJ316
	FN13=FN**CON2	BESJ317
	RTARY=RTZ*FN13	BESJ318
	ARY=-RTARY*RTARY	BESJ319
	AZ32=AZ*RTZ*CON1	BESJ320
	ACZ=FN*AZ32	BESJ321
	IF(Z.LE.0.) GO TO 27	BESJ322
C		BESJ323
C	TEST FOR UNDERFLOW, 1.E-280=EXP(-644.), ONE WORD LENGTH	BESJ324
C	UP FROM UNDERFLOW LIMIT OF CDC 6600	BESJ325
C		BESJ326
	IF(ACZ.GT.ELIM2) GO TO 180	BESJ327
	ARY=-ARY	BESJ328
27	PHI=SQRT(SQRT(SA+SA+SA+SA))	BESJ329
C		BESJ330
C	B(ZETA) FOR S=0	BESJ331
C		BESJ332
	KB=KMAX(5)	BESJ333
	KLAST=KB-1	BESJ334
	SB=BETA(KB,1)	BESJ335
	DO 23 K=1,KLAST	BESJ336
	KB=KB-1	BESJ337
	SB=SB*W2+BETA(KB,1)	BESJ338
23	CONTINUE	BESJ339
	KSP1=1	BESJ340
	FN2=FN*FN	BESJ341
	RFN2=1./FN2	BESJ342
	RDEN=1.	BESJ343
	ASUM=1.	BESJ344
	RELB=TOL*ABS(SB)	BESJ345
	BSUM=SB	BESJ346
	DO 25 KS=1,4	BESJ347
	KSP1=KSP1+1	BESJ348
	RDEN=RDEN*RFN2	BESJ349

Figure A3. (Sheet 9 of 25)

C		BESJ350
C	A(ZETA) AND B(ZETA) FOR S=1,2,3,4	BESJ351
C		BESJ352
	KB=KMAX(5-KS)	BESJ353
	KLAST=KB-1	BESJ354
	SA=ALFA(KB,KS)	BESJ355
	SB=BETA(KB,KSP1)	BESJ356
	DO 26 K=1,KLAST	BESJ357
	KB=KB-1	BESJ358
	SA=SA*W2+ALFA(KB,KS)	BESJ359
	SB=SB*W2+BETA(KB,KSP1)	BESJ360
26	CONTINUE	BESJ361
	TA=SA*RDEN	BESJ362
	TB=SB*RDEN	BESJ363
	ASUM=ASUM+TA	BESJ364
	BSUM=BSUM+TB	BESJ365
	IF (ABS(TA).LE.TOL.AND.ABS(TB).LE.RELB) GO TO 152	BESJ366
25	CONTINUE	BESJ367
152	CONTINUE	BESJ368
	BSUM=BSUM/(FN*FN13)	BESJ369
	GO TO 400	BESJ370
C		BESJ371
200	CONTINUE	BESJ372
	TAU=1./RA	BESJ373
	T2=1./W2	BESJ374
	IF(W2.GE.0.) GO TO 30	BESJ375
C		BESJ376
C	CASES FOR (X/FN).GT.SQRT(1.2775)	BESJ377
C		BESJ378
	AZ32=ABS(RA-ATAN(RA))	BESJ379
	ACZ=AZ32*FN	BESJ380
	CZ=-ACZ	BESJ381
	Z32=1.5*AZ32	BESJ382
	RTZ=Z32**CON2	BESJ383
	FN13=FN**CON2	BESJ384
	RTARY=RTZ*FN13	BESJ385
	ARY=-RTARY*RTARY	BESJ386
	GO TO 150	BESJ387
30	CONTINUE	BESJ388
C		BESJ389
C	CASES FOR (X/FN).LT.SQRT(0.7225)	BESJ390
C		BESJ391
	AZ32=ABS(ALOG((1.+RA)/XX) -RA)	BESJ392
C		BESJ393
C	TEST FOR UNDERFLOW, 1.E-280 = EXP(-644.), ONE WORD LENGTH	BESJ394
C	UP FROM UNDERFLOW LIMIT OF CDC 6600	BESJ395
C		BESJ396
	ACZ=AZ32*FN	BESJ397
	CZ=ACZ	BESJ398
	IF(ACZ.GT.ELIM2) GO TO 180	BESJ399
	Z32=1.5*AZ32	BESJ400
	RTZ=Z32**CON2	BESJ401
	FN13=FN**CON2	BESJ402
	RTARY=RTZ*FN13	BESJ403
	ARY=RTARY*RTARY	BESJ404

Figure A3. (Sheet 10 of 25)

150	CONTINUE	BESJ405
	PHI=SQRT((RTZ+RTZ)*TAU)	BESJ406
	TB=1.	BESJ407
	ASUM=1.	BESJ408
	TFN=TAU/FN	BESJ409
	UPOL(2)=(C(1,1)*T2+C(2,1))*TFN	BESJ410
	RCZ=CON1/CZ	BESJ411
	CRZ32=CON548*RCZ	BESJ412
	BSUM=UPOL(2)+CRZ32	BESJ413
	RELB=TOL*ABS(BSUM)	BESJ414
	AP=TFN	BESJ415
	KS=0	BESJ416
	KP1=2	BESJ417
	RZDEN=RCZ	BESJ418
	DO 155 LR=2,8,2	BESJ419
C		BESJ420
C	COMPUTE TWO U POLYNOMIALS FOR NEXT A(ZETA) AND B(ZETA)	BESJ421
C		BESJ422
	LRP1=LR+1	BESJ423
	DO 101 K=LR,LRP1	BESJ424
	KS=KS+1	BESJ425
	KP1=KP1+1	BESJ426
	S1=C(1,K)	BESJ427
	DO 102 J=2,KP1	BESJ428
	S1=S1*T2+C(J,K)	BESJ429
102	CONTINUE	BESJ430
	AP=AP*TFN	BESJ431
	UPOL(KP1)=AP*S1	BESJ432
	CR(KS)=BR(KS)*RZDEN	BESJ433
	RZDEN=RZDEN*RCZ	BESJ434
	DR(KS)=AR(KS)*RZDEN	BESJ435
101	CONTINUE	BESJ436
	SUMA=UPOL(LRP1)	BESJ437
	SUMB=UPOL(LR+2)+UPOL(LRP1)*CRZ32	BESJ438
	JU=LRP1	BESJ439
	DO 151 JR=1,LR	BESJ440
	JU=JU-1	BESJ441
	SUMA=SUMA+CR(JR)*UPOL(JU)	BESJ442
	SUMB=SUMB+DR(JR)*UPOL(JU)	BESJ443
151	CONTINUE	BESJ444
	TB=-TB	BESJ445
	IF(W2.GT.0.) TB=ABS(TB)	BESJ446
	ASUM=ASUM+SUMA*TB	BESJ447
	BSUM=BSUM+SUMB*TB	BESJ448
	IF(ABS(SUMA).LE.TOL.AND.ABS(SUMB).LE.RELB) GO TO 165	BESJ449
155	CONTINUE	BESJ450
165	TB=RTARY	BESJ451
	IF(W2.GT.0.) TB=-TB	BESJ452
	BSUM=BSUM/TB	BESJ453
C		BESJ454
400	CONTINUE	BESJ455
	CALL JAIRY(ARY,RTARY,ACZ,AI,DAI)	BESJ456
	TEMP(IS)=PHI*(AI*ASUM+DAI*BSUM)/FN13	BESJ457
	GO TO (401,202,650), IS	BESJ458
402	TEMP(1)=TEMP(3)	BESJ459

Figure A3. (Sheet 11 of 25)

	KT=1	BESJ460
401	IS=2	BESJ461
	DFN=DFN-1.D+0	BESJ462
	FN=DFN	BESJ463
	GO TO 130	BESJ464
C		BESJ465
C	SERIES FOR (X/2)**2.LE.NU+1	BESJ466
C		BESJ467
134	CONTINUE	BESJ468
	GLN=GAMLN(FNP1)	BESJ469
	ARG=FN*X02L-GLN	BESJ470
	IF(ARG.LT.-ELIM1) GO TO 123	BESJ471
	EARG=EXP(ARG)	BESJ472
300	CONTINUE	BESJ473
	S=1.	BESJ474
	AK=3.	BESJ475
	T2=1.	BESJ476
	T=1.	BESJ477
	S1=FN	BESJ478
	DO 125 K=1,17	BESJ479
	S2=T2+S1	BESJ480
	T=-T*SX02/S2	BESJ481
	S=S+T	BESJ482
	IF(ABS(T).LT.TOL) GO TO 127	BESJ483
	T2=T2+AK	BESJ484
	AK=AK+2.	BESJ485
	S1=S1+FN	BESJ486
125	CONTINUE	BESJ487
127	CONTINUE	BESJ488
	TEMP(IS)=S*EARG	BESJ489
	GO TO (301,202,600), IS	BESJ490
301	EARG=EARG*FN/X02	BESJ491
	DFN=DFN-1.D+0	BESJ492
	FN=DFN	BESJ493
	IS=2	BESJ494
	GO TO 300	BESJ495
C		BESJ496
C	SET UNDERFLOW VALUE AND UPDATE PARAMETERS	BESJ497
C		BESJ498
180	Y(NN)=0.	BESJ499
	NN=NN-1	BESJ500
	DFN=DFN-1.D+0	BESJ501
	FN=DFN	BESJ502
	IF (NN-1) 170,171,130	BESJ 503
171	KT=2	BESJ504
	IS=2	BESJ505
	GO TO 130	BESJ506
123	Y(NN)=0.	BESJ507
	NN=NN-1	BESJ508
	FNP1=FN	BESJ509
	DFN=DFN-1.D+0	BESJ510
	FN=DFN	BESJ511
	IF(NN-1) 170,172,173	BESJ512
172	KT=2	BESJ513
	IS=2	BESJ514

Figure A3. (Sheet 12 of 25)

173	IF(SX02.LE.FNP1) GO TO 133	BESJ515
	GO TO 130	BESJ516
133	ARG=ARG-X02L+ALOG(FNP1)	BESJ517
	IF(ARG.LT.-ELIM1) GO TO 123	BESJ518
	GO TO 134	BESJ519
170	NZ=N-NN	BESJ520
	RETURN	BESJ521
C		BESJ522
C	BACKWARD RECURSION SECTION	BESJ523
C		BESJ524
202	CONTINUE	BESJ525
	NZ=N-NN	BESJ526
	IF(KT.EQ.2) GO TO 250	BESJ527
203	CONTINUE	BESJ528
C	BACKWARD RECUR FROM INDEX ALPHA+NN-1 TO ALPHA	BESJ529
	Y(NN)=TEMP(1)	BESJ530
	Y(NN-1)=TEMP(2)	BESJ531
	IF(NN.EQ.2) RETURN	BESJ532
	DX=X	BESJ533
	TRX=2.D+0/DX	BESJ534
	DTM=DFN*TRX	BESJ535
	TM=DTM	BESJ536
	K=NN+1	BESJ537
	DO 230 I=3,NN	BESJ538
	K=K-1	BESJ539
	Y(K-2)=TM*Y(K-1)-Y(K)	BESJ540
	DTM=DTM-TRX	BESJ541
	TM=DTM	BESJ542
230	CONTINUE	BESJ543
	RETURN	BESJ544
250	Y(1)=TEMP(2)	BESJ545
	RETURN	BESJ546
C		BESJ547
C	ASYMPTOTIC EXPANSION FOR X TO INFINITY WITH FORWARD RECURSION IN	BESJ548
C	OSCILLATORY REGION X.GT.MAX(20, NU), PROVIDED THE LAST MEMBER	BESJ549
C	OF THE SEQUENCE IS ALSO IN THE REGION.	BESJ550
C		BESJ551
500	CONTINUE	BESJ552
	IN=ALPHA-TAU+2.	BESJ553
	IF(IN.LE.0) GO TO 502	BESJ554
	INP1=IN+1	BESJ555
	DALPHA=ALPHA-FLOAT(INP1)	BESJ556
	KT=1	BESJ557
	GO TO 511	BESJ558
502	DALPHA=ALPHA	BESJ559
	IN=0	BESJ560
511	IS=KT	BESJ561
512	ARG=X-PIDT*DALPHA-PDF	BESJ562
	SA=SIN(ARG)	BESJ563
	SB=COS(ARG)	BESJ564
	RA=RTTP/RTX	BESJ565
	ETX=8.*X	BESJ566
503	DX=DALPHA	BESJ567
	DX=DX+DX	BESJ568
	DTM=DX*DX	BESJ569

Figure A3. (Sheet 13 of 25)

T2=DTM-1.D+0	BESJ570
T2=T2/ETX	BESJ571
S2=T2	BESJ572
RELB=TOL*ABS(T2)	BESJ573
T1=ETX	BESJ574
S1=1.	BESJ575
FN=1.	BESJ576
AK=8.	BESJ577
DO 504 K=1,13	BESJ578
T1=T1+ETX	BESJ579
FN=FN+AK	BESJ580
DX=FN	BESJ581
TRX=DTM-DX	BESJ582
AP=TRX	BESJ583
T2=-T2*AP/T1	BESJ584
S1=S1+T2	BESJ585
T1=T1+ETX	BESJ586
AK=AK+8.	BESJ587
FN=FN+AK	BESJ588
DX=FN	BESJ589
TRX=DTM-DX	BESJ590
AP=TRX	BESJ591
T2= T2*AP/T1	BESJ592
S2=S2+T2	BESJ593
IF(ABS(T2).LE.RELB) GO TO 505	BESJ594
AK=AK+8.	BESJ595
504 CONTINUE	BESJ596
505 TEMP(IS)=RA*(S1*SB-S2*SA)	BESJ597
GO TO (506,507),IS	BESJ598
506 DALPHA=DALPHA+1.	BESJ599
IS=2	BESJ600
TB=SA	BESJ601
SA=-SB	BESJ602
SB=TB	BESJ603
GO TO 503	BESJ604
C	BESJ605
C FORWARD RECURSION SECTION	BESJ606
C	BESJ607
507 IF(KT.EQ.2) GO TO 250	BESJ608
S1=TEMP(1)	BESJ609
S2=TEMP(2)	BESJ610
TX=2./X	BESJ611
TM=DALPHA*TX	BESJ612
IF(IN.EQ.0) GO TO 520	BESJ613
C	BESJ614
C FORWARD RECUR TO INDEX ALPHA	BESJ615
C	BESJ616
DO 510 I=1,IN	BESJ617
S=S2	BESJ618
S2=TM*S2-S1	BESJ619
TM=TM+TX	BESJ620
S1=S	BESJ621
510 CONTINUE	BESJ622
IF(NN.EQ.1) GO TO 535	BESJ623
S=S2	BESJ624

Figure A3. (Sheet 14 of 25)

	S2=TM>S2-S1	BESJ625
	TM=TM+TX	BESJ626
	S1=S	BESJ627
520	CONTINUE	BESJ628
C		BESJ629
C	FORWARD RECUR FROM INDEX ALPHA TO ALPHA+N-1	BESJ630
C		BESJ631
	Y(1)=S1	BESJ632
	Y(2)=S2	BESJ633
	IF(NN.EQ.2) RETURN	BESJ634
	DO 530 I=3,NN	BESJ635
	Y(I)=TM*Y(I-1)-Y(I-2)	BESJ636
	TM=TM+TX	BESJ637
530	CONTINUE	BESJ638
	RETURN	BESJ639
535	Y(1)=S2	BESJ640
	RETURN	BESJ641
C		BESJ642
C	BACKWARD RECURSION WITH NORMALIZATION BY	BESJ643
C	ASYMPTOTIC EXPANSION FOR NU TO INFINITY OR POWER SERIES.	BESJ644
C		BESJ645
600	CONTINUE	BESJ646
C	COMPUTATION OF LAST ORDER FOR SERIES NORMALIZATION	BESJ647
	KM=AMAX1(3,-FN,0.)	BESJ648
	TFN=FN+FLOAT(KM)	BESJ649
	TA=(GLN+TFN-0.9189385332-0.0833333333/TFN)/(TFN+0.5)	BESJ650
	TA=X02L-TA	BESJ651
	TB=-(1.-1.5/TFN)/TFN	BESJ652
	IN=CE/(-TA+SQRT(TA*TA-CE*TB))+1.5	BESJ653
	IN=IN+KM	BESJ654
	GO TO 603	BESJ655
650	CONTINUE	BESJ656
C	COMPUTATION OF LAST ORDER FOR ASYMPTOTIC EXPANSION NORMALIZATION	BESJ657
	GLN=AZ32+RA	BESJ658
	IF(ARY.GT.30.) GO TO 675	BESJ659
	RDEN=(PP(4)*ARY+PP(3))*ARY+1.	BESJ660
	RZDEN=PP(1)+PP(2)*ARY	BESJ661
	TA=RZDEN/RDEN	BESJ662
	IF(W2.LT.0.10) GO TO 651	BESJ663
	TB=GLN/RTARY	BESJ664
	GO TO 677	BESJ665
651	TB=(1.259921049+0.1679894730*W2)/FN13	BESJ666
	GO TO 677	BESJ667
675	CONTINUE	BESJ668
	TA=CON1*TCE/ACZ	BESJ669
	TA=((0.0493827160*TA-0.1111111111)*TA+0.6666666667)*TA*ARY	BESJ670
	IF(W2.LT.0.10) GO TO 651	BESJ671
	TB=GLN/RTARY	BESJ672
677	IN=TA/TB+1.5	BESJ673
	IF(IN.GT.INLIM) GO TO 402	BESJ674
603	DX=FLOAT(IN)	BESJ675
	DTM=DFN+DX	BESJ676
	DX=X	BESJ677
	TRX=2.D+0/DX	BESJ678
	DTM=DTM*TRX	BESJ679

Figure A3. (Sheet 15 of 25)

	TM=DTM	BESJ680
	TA=0.	BESJ681
	TB=TOL	BESJ682
	KK=1	BESJ683
	605 CONTINUE	BESJ684
C		BESJ685
C	BACKWARD RECUR UNINDEXED	BESJ686
C		BESJ687
	DO 601 I=1,IN	BESJ688
	S=TB	BESJ689
	TB=TM*TB-TA	BESJ690
	TA=S	BESJ691
	DTM=DTM-TRX	BESJ692
	TM=DTM	BESJ693
	601 CONTINUE	BESJ694
C	NORMALIZATION	BESJ695
	IF(KK.NE.1) GO TO 604	BESJ696
	TA=(TA/TB)*TEMP(3)	BESJ697
	TB=TEMP(3)	BESJ698
	KK=2	BESJ699
	IN=NS	BESJ700
	IF(NS.NE.0) GO TO 605	BESJ701
604	Y(NN)=TB	BESJ702
615	NZ=N-NN	BESJ703
	IF(NN.EQ.1) RETURN	BESJ704
	S=TB	BESJ705
	TB=TM*TB-TA	BESJ706
	TA=S	BESJ707
	DTM=DTM-TRX	BESJ708
	TM=DTM	BESJ709
	K=NN-1	BESJ710
	Y(K)=TB	BESJ711
	IF(NN.EQ.2) RETURN	BESJ712
	KM=K-1	BESJ713
C		BESJ714
C	BACKWARD RECUR INDEXED	BESJ715
C		BESJ716
	DO 602 I=1,KM	BESJ717
	Y(K-1)=TM*Y(K)-Y(K+1)	BESJ718
	DTM=DTM-TRX	BESJ719
	TM=DTM	BESJ720
	K=K-1	BESJ721
602	CONTINUE	BESJ722
	RETURN	BESJ723
C		BESJ724
C		BESJ725
C		BESJ726
	91 CONTINUE	BESJ727
	NZ=-2	BESJ728
	RETURN	BESJ729
	92 CONTINUE	BESJ730
	NZ=-3	BESJ731
	RETURN	BESJ732
	93 CONTINUE	BESJ733
	NZ=-1	BESJ734

Figure A3. (Sheet 16 of 25)

```

RETURN
END
SUBROUTINE JAIRY(X,RX,C,AI,DAI)
C -----
C CDC 6600 ROUTINE 1-2-74
C JAIRY COMPUTES THE AIRY FUNCTION AI(X)
C AND ITS DERIVATIVE DAI(X) FOR JBESS
C
C INPUT: X - ARGUMENT, COMPUTED BY JBESS, X UNRESTRICTED
C RX - RX=SQRT(ABS(X)), COMPUTED BY JBESS
C C - C=2.*(ABS(X)**1.5)/3., COMPUTED BY JBESS
C OUTPUT: AI - VALUE OF FUNCTION AI(X)
C DAI - VALUE OF THE DERIVATIVE DAI(X)
C
C WRITTEN BY D.E. AMOS, S.L. DANIEL & M.K WESTON
C -----
DIMENSION AK1(14),AK2(23),AK3(14)
DIMENSION AJP(19),AJN(19),A(15),B(15)
DIMENSION DAK1(14),DAK2(24),DAK3(14)
DIMENSION DAJP(19),DAJN(19),DA(15),DB(15)
DATA N1,N2,N3,N4/14,23,19,15/
DATA M1,M2,M3,M4/12,21,17,13/
DATA FPI12,CON1,CON2,CON3,CON4,CON5/
1 1.3089969389958E+00, 6.6666666666667E-01, 5.0315471619678E+00,
2 3.8000458986729E-01, 8.3333333333333E-01, 8.6602540378444E-01/
DATA AK1(1) / 2.2042309098779E-01/,
1 AK1(2) /-1.2529024278770E-01/, AK1(3) / 1.0388116335919E-02/,
2 AK1(4) / 8.2284415200634E-04/, AK1(5) /-2.3461434589123E-04/,
3 AK1(6) / 1.6382428017212E-05/, AK1(7) / 3.0690258957319E-07/,
4 AK1(8) /-1.2962199935933E-07/, AK1(9) / 8.2290815882367E-09/,
5 AK1(10)/ 1.5396396862330E-11/, AK1(11)/-3.3916546561568E-11/,
6 AK1(12)/ 2.0325325742363E-12/, AK1(13)/-1.1067954609788E-14/,
7 AK1(14)/-5.1616949778508E-15/
DATA AK2(1) / 2.7436615086960E-01/,
1 AK2(2) / 5.3979096973690E-03/, AK2(3) /-1.5733922062119E-03/,
2 AK2(4) / 4.2742752824875E-04/, AK2(5) /-1.1212491739992E-04/,
3 AK2(6) / 2.8876317131890E-05/, AK2(7) /-7.3680422537055E-06/,
4 AK2(8) / 1.8729020974102E-06/, AK2(9) /-4.7589279396229E-07/,
5 AK2(10)/ 1.2113041695591E-07/, AK2(11)/-3.0924537427061E-08/,
6 AK2(12)/ 7.9245470528265E-09/, AK2(13)/-2.0390244716791E-09/,
7 AK2(14)/ 5.2686305659574E-10/, AK2(15)/-1.3670476763957E-10/,
9 AK2(16)/ 3.5614103901371E-11/, AK2(17)/-9.3138829654843E-12/,
9 AK2(18)/ 2.4446445047364E-12/, AK2(19)/-6.4384026199096E-13/,
1 AK2(20)/ 1.7010603055935E-13/, AK2(21)/-4.5076010450328E-14/,
2 AK2(22)/ 1.1977479916481E-14/, AK2(23)/-3.1907704086507E-15/
DATA AK3(1) / 2.8027144734079E-01/,
1 AK3(2) /-1.7812704284438E-03/, AK3(3) / 4.0342257962900E-05/,
2 AK3(4) /-1.6324996526900E-06/, AK3(5) / 9.2118148247677E-08/,
3 AK3(6) /-6.5229433022916E-09/, AK3(7) / 5.4713840457655E-10/,
4 AK3(8) /-5.2440825180026E-11/, AK3(9) / 5.6047790411721E-12/,
5 AK3(10)/-6.5637524463931E-13/, AK3(11)/ 8.3128576196625E-14/,
6 AK3(12)/-1.1270513469106E-14/, AK3(13)/ 1.6226797659813E-15/,
7 AK3(14)/-2.4648032431243E-16/
DATA AJP(1) / 7.7895296643758E-02/,
1 AJP(2) /-1.8435636345680E-01/, AJP(3) / 3.0141260521617E-02/,

```

Figure A3. (Sheet 17 of 25)

2	AJP(4) / 3.0534272427761E-02/	AJP(5) / -4.9542470251308E-03/	AIRY54
3	AJP(6) / -1.7274955256395E-03/	AJP(7) / 2.4313763783919E-04/	AIRY55
4	AJP(8) / 5.0456477751708E-05/	AJP(9) / -6.1631658269521E-06/	AIRY56
5	AJP(10) / -9.0398674551077E-07/	AJP(11) / 9.7024377835588E-08/	AIRY57
6	AJP(12) / 1.0963945330520E-08/	AJP(13) / -1.0471633058877E-09/	AIRY58
7	AJP(14) / -9.6035944134465E-11/	AJP(15) / 8.2535878945413E-12/	AIRY59
8	AJP(16) / 6.3612343901877E-13/	AJP(17) / -4.9662961411602E-14/	AIRY60
9	AJP(18) / -3.2981028892962E-15/	AJP(19) / 2.3579825203110E-16/	AIRY61
	DATA AJN(1) / 3.8049788761724E-02/		AIRY62
1	AJN(2) / -2.4531954184555E-01/	AJN(3) / 1.6582062370270E-01/	AIRY63
2	AJN(4) / 7.4933004581879E-02/	AJN(5) / -2.6347628810664E-02/	AIRY64
3	AJN(6) / -5.9253559730498E-03/	AJN(7) / 1.4474440958980E-03/	AIRY65
4	AJN(8) / 2.1831183132222E-04/	AJN(9) / -4.1066207768030E-05/	AIRY66
5	AJN(10) / -4.6687499417177E-06/	AJN(11) / 7.1521886727716E-07/	AIRY67
6	AJN(12) / 6.5296477085463E-08/	AJN(13) / -8.4428402756595E-09/	AIRY68
7	AJN(14) / -6.4418615897698E-10/	AJN(15) / 7.2080228650528E-11/	AIRY69
8	AJN(16) / 4.7246543171785E-12/	AJN(17) / -4.6602263254704E-13/	AIRY70
9	AJN(18) / -2.6776271038919E-14/	AJN(19) / 2.3616131657002E-15/	AIRY71
	DATA A(1) / 4.9027542474279E-01/	A(2) / 1.5764727794620E-03/	AIRY72
1	A(3) / -9.6619596314031E-05/	A(4) / 1.3591608026882E-07/	AIRY73
2	A(5) / 2.9815734265486E-07/	A(6) / -1.8682476755998E-08/	AIRY74
3	A(7) / -1.0368573766714E-09/	A(8) / 3.2866081843433E-10/	AIRY75
4	A(9) / -2.5709141063278E-11/	A(10) / -2.3235765530068E-12/	AIRY76
5	A(11) / 9.5752327904826E-13/	A(12) / -1.2034082804972E-13/	AIRY77
6	A(13) / -2.9090771677072E-15/	A(14) / 4.5565645458015E-15/	AIRY78
7	A(15) / -9.9900387481026E-16/		AIRY79
	DATA B(1) / 2.7859355280308E-01/	B(2) / -3.5291569188258E-03/	AIRY80
1	B(3) / -2.3114967738499E-05/	B(4) / 4.7131784226356E-06/	AIRY81
2	B(5) / -1.1241590793133E-07/	B(6) / -2.0010030118434E-08/	AIRY82
3	B(7) / 2.6094807530219E-09/	B(8) / -3.5509813610122E-11/	AIRY83
4	B(9) / -3.5084997842388E-11/	B(10) / 5.8300718795420E-12/	AIRY84
5	B(11) / -2.0464482875333E-13/	B(12) / -1.1052917947674E-13/	AIRY85
6	B(13) / 2.8772477803878E-14/	B(14) / -2.8820511100994E-15/	AIRY86
7	B(15) / -3.3265631169617E-16/		AIRY87
	DATA N1D,N2D,N3D,N4D/14,24,19,15/		AIRY88
	DATA M1D,M2D,M3D,M4D/12,22,17,13/		AIRY89
	DATA DAK1(1) / 2.0456784230789E-01/		AIRY90
1	DAK1(2) / -8.6132273990566E-02/	DAK1(3) / -8.4984580098929E-03/	AIRY91
2	DAK1(4) / 3.1218349155629E-03/	DAK1(5) / -2.7001648982943E-04/	AIRY92
3	DAK1(6) / -6.3563629867939E-06/	DAK1(7) / 3.0239771240951E-06/	AIRY93
4	DAK1(8) / -2.1831119533009E-07/	DAK1(9) / -5.3619428933283E-10/	AIRY94
5	DAK1(10) / 1.1309803562231E-09/	DAK1(11) / -7.4302383462907E-11/	AIRY95
6	DAK1(12) / 4.2880417082689E-13/	DAK1(13) / 2.2381092575454E-13/	AIRY96
7	DAK1(14) / -1.3914013564118E-14/		AIRY97
	DATA DAK2(1) / 2.9333234388323E-01/		AIRY98
1	DAK2(2) / -8.0619678474311E-03/	DAK2(3) / 2.4254017233314E-03/	AIRY99
2	DAK2(4) / -6.8229754885024E-04/	DAK2(5) / 1.8578642775118E-04/	AIRY100
3	DAK2(6) / -4.9745744768406E-05/	DAK2(7) / 1.3209068123950E-05/	AIRY101
4	DAK2(8) / -3.4952824044494E-06/	DAK2(9) / 9.2436245107884E-07/	AIRY102
5	DAK2(10) / -2.4473267152187E-07/	DAK2(11) / 6.4930783764891E-08/	AIRY103
6	DAK2(12) / -1.7271762150154E-08/	DAK2(13) / 4.6072576360466E-09/	AIRY104
7	DAK2(14) / -1.2324905529155E-09/	DAK2(15) / 3.3062040948810E-10/	AIRY105
8	DAK2(16) / -8.8925209977240E-11/	DAK2(17) / 2.3977331987830E-11/	AIRY106
9	DAK2(18) / -6.4801392115345E-12/	DAK2(19) / 1.7551013202373E-12/	AIRY107
1	DAK2(20) / -4.7630382983364E-13/	DAK2(21) / 1.2949824110081E-13/	AIRY108

Figure A3. (Sheet 18 of 25)

```

2 DAK2(22)/-3.5267962221043E-14/, DAK2(23)/ 9.6200515158592E-15/, AIRY109
3 DAK2(24)/-2.6278691434229E-15/ AIRY110
DATA DAK3(1) / 2.8467582881135E-01/, AIRY111
1 DAK3(2) / 2.5307307261908E-03/, DAK3(3) /-4.8348113033798E-05/, AIRY112
2 DAK3(4) / 1.8490728394634E-06/, DAK3(5) /-1.0141849117858E-07/, AIRY113
3 DAK3(6) / 7.0592563445715E-09/, DAK3(7) /-5.8532529140038E-10/, AIRY114
4 DAK3(8) / 5.5635768883134E-11/, DAK3(9) /-5.9088909477950E-12/, AIRY115
5 DAK3(10)/ 6.8857435378444E-13/, DAK3(11)/-8.6858825645219E-14/, AIRY116
6 DAK3(12)/ 1.1737476261721E-14/, DAK3(13)/-1.6852314651092E-15/, AIRY117
7 DAK3(14)/ 2.5537477309706E-16/ AIRY118
DATA DAJP(1) / 6.5321913131146E-02/, AIRY119
1 DAJP(2) /-1.2026293368882E-01/, DAJP(3) / 9.7801023626382E-03/, AIRY120
2 DAJP(4) / 1.6794842923050E-02/, DAJP(5) /-1.9714614018213E-03/, AIRY121
3 DAJP(6) /-8.4556029509887E-04/, DAJP(7) / 9.4288962070198E-05/, AIRY122
4 DAJP(8) / 2.2582786094548E-05/, DAJP(9) /-2.2906787091599E-06/, AIRY123
5 DAJP(10)/-3.7634399113692E-07/, DAJP(11)/ 3.4566393355956E-08/, AIRY124
6 DAJP(12)/ 4.2961133200301E-09/, DAJP(13)/-3.5867369121499E-10/, AIRY125
7 DAJP(14)/-3.5724588136190E-11/, DAJP(15)/ 2.7269609106634E-12/, AIRY126
8 DAJP(16)/ 2.2612065309577E-13/, DAJP(17)/-1.5876320523830E-14/, AIRY127
9 DAJP(18)/-1.1260437448512E-15/, DAJP(19)/ 7.3132752951537E-17/ AIRY128
DATA DAJN(1) / 1.0859453963297E-02/, AIRY129
1 DAJN(2) / 8.5331319485709E-02/, DAJN(3) /-3.1527706811306E-01/, AIRY130
2 DAJN(4) /-8.7842072529426E-02/, DAJN(5) / 5.5325190697605E-02/, AIRY131
3 DAJN(6) / 9.4167406050324E-03/, DAJN(7) /-3.3218702601900E-03/, BEJS132
4 DAJN(8) /-4.1115734315683E-04/, DAJN(9) / 1.0129732689135E-04/, AIRY133
5 DAJN(10)/ 9.8763368220840E-06/, DAJN(11)/-1.8731296981239E-06/, AIRY134
6 DAJN(12)/-1.5079850013147E-07/, DAJN(13)/ 2.3268766952539E-08/, AIRY135
7 DAJN(14)/ 1.5959991741922E-09/, DAJN(15)/-2.0766592266838E-10/, AIRY136
8 DAJN(16)/-1.2410335050030E-11/, DAJN(17)/ 1.3963176533104E-12/, AIRY137
9 DAJN(18)/ 7.3940097115574E-14/, DAJN(19)/-7.3288747562750E-15/ AIRY137
DATA DA(1) / 4.9162732110460E-01/, DA(2) / 3.1116493042749E-03/, AIRY139
1 DA(3) / 8.2314076285408E-05/, DA(4) /-4.6176977617214E-06/, AIRY140
2 DA(5) /-6.1315888053463E-08/, DA(6) / 2.8729580465652E-08/, AIRY141
3 DA(7) /-1.8195971537212E-09/, DA(8) /-1.4475282664204E-10/, AIRY142
4 DA(9) / 4.5372404342042E-11/, DA(10)/-3.9965506584722E-12/, AIRY143
5 DA(11)/-3.2408911983032E-13/, DA(12)/ 1.6209895256874E-13/, AIRY144
6 DA(13)/-2.4076524797406E-14/, DA(14)/ 1.6938481128449E-16/, AIRY145
7 DA(15)/ 8.1790078647740E-16/ AIRY146
DATA DB(1) /-2.7757135694423E-01/, DB(2) / 4.4421283341992E-03/, AIRY147
1 DB(3) /-8.4232852219009E-05/, DB(4) /-2.5804031841871E-06/, AIRY148
2 DB(5) / 3.4238972021762E-07/, DB(6) /-6.2428689470978E-09/, AIRY149
3 DB(7) /-2.3637783684458E-09/, DB(8) / 3.1699104265667E-10/, AIRY150
4 DB(9) /-4.4099569165819E-12/, DB(10)/-5.1867422109358E-12/, AIRY151
5 DB(11)/ 9.6487401513702E-13/, DB(12)/-4.9019057660871E-14/, AIRY152
6 DB(13)/-1.7725343067811E-14/, DB(14)/ 5.5595061044266E-15/, AIRY153
7 DB(15)/-7.1179333757953E-16/ AIRY154
----- AIRY155
IF(X.LT.0.) GO TO 300 AIRY156
IF(C.GT.5.) GO TO 200 AIRY157
IF(X.GT.1.2) GO TO 150 AIRY158
T=(X+X-1.2)*CON4 AIRY159
T1 = T + T AIRY160
J=N1 AIRY161
F1=AK1(J) AIRY162
F2=0. AIRY163

```

Figure A3. (Sheet 19 of 25)

DO 105 I=1,M1	AIRY164
J=J-1	AIRY165
TEMP1=F1	AIRY166
F1=TT*F1-F2+AK1(J)	AIRY167
F2=TEMP1	AIRY168
105 CONTINUE	AIRY169
AI=T*F1-F2+AK1(1)	AIRY170
C	AIRY171
J=N1D	AIRY172
F1=DAK1(J)	AIRY173
F2=0.	AIRY174
DO 106 I=1,M1D	AIRY175
J=J-1	AIRY176
TEMP1=F1	AIRY177
F1=TT*F1-F2+DAK1(J)	AIRY178
F2=TEMP1	AIRY179
106 CONTINUE	AIRY180
DAI=-(T*F1-F2+DAK1(1))	AIRY181
RETURN	AIRY182
C	AIRY183
150 CONTINUE	AIRY184
T=(X+X-CON2)*CON3	AIRY185
TT = T + T	AIRY186
J=N2	AIRY187
F1=AK2(J)	AIRY188
F2=0.	AIRY189
DO 155 I=1,M2	AIRY190
J=J-1	AIRY191
TEMP1=F1	AIRY192
F1=TT*F1-F2+AK2(J)	AIRY193
F2=TEMP1	AIRY194
155 CONTINUE	AIRY195
RTRX=SQRT(RX)	AIRY196
EC=EXP(-C)	AIRY197
AI=EC*(T*F1-F2+AK2(1))/RTRX	AIRY198
J=N2D	AIRY199
F1=DAK2(J)	AIRY200
F2=0.	AIRY201
DO 156 I=1,M2D	AIRY202
J=J-1	AIRY203
TEMP1=F1	AIRY204
F1=TT*F1-F2+DAK2(J)	AIRY205
F2=TEMP1	AIRY206
156 CONTINUE	AIRY207
DAI=-EC*(T*F1-F2+DAK2(1))*RTRX	AIRY208
RETURN	AIRY209
C	AIRY210
200 CONTINUE	AIRY211
T=10./C-1.	AIRY212
TT=T+T	AIRY213
J=N1	AIRY214
F1=AK3(J)	AIRY215
F2=0.	AIRY216
DO 205 I=1,M1	AIRY217
J=J-1	AIRY218

Figure A3. (Sheet 20 of 25)

	TEMP1=F1	AIRY219
	F1=TT*F1-F2+AK3(J)	AIRY220
	F2=TEMP1	AIRY221
205	CONTINUE	AIRY222
	RTRX=SQRT(RX)	AIRY223
	EC=EXP(-C)	AIRY224
	AI=EC*(T*F1-F2+AK3(1))/RTRX	AIRY225
	J=N1D	AIRY226
	F1=DAK3(J)	AIRY227
	F2=0.	AIRY228
	DO 206 I=1,M1D	AIRY229
	J=J-1	AIRY230
	TEMP1=F1	AIRY231
	F1=TT*F1-F2+DAK3(J)	AIRY232
	F2=TEMP1	AIRY233
206	CONTINUE	AIRY234
	DAI=-RTRX*EC*(T*F1-F2+DAK3(1))	AIRY235
	RETURN	AIRY236
C		AIRY237
300	CONTINUE	AIRY238
	IF(C.GT.5.) GO TO 350	AIRY239
	T=.4*C-1.	AIRY240
	TT=T+T	AIRY241
	J=N3	AIRY242
	F1=AJP(J)	AIRY243
	E1=AJN(J)	AIRY244
	F2=0.	AIRY245
	E2=0.	AIRY246
	DO 305 I=1,M3	AIRY247
	J=J-1	AIRY248
	TEMP1=F1	AIRY249
	TEMP2=E1	AIRY250
	F1=TT*F1-F2+AJP(J)	AIRY251
	E1=TT*E1-E2+AJN(J)	AIRY252
	F2=TEMP1	AIRY253
	E2=TEMP2	AIRY254
305	CONTINUE	AIRY255
	AI=(T*E1-E2+AJN(1))-X*(T*F1-F2+AJP(1))	AIRY256
	J=N3D	AIRY257
	F1=DAJP(J)	AIRY258
	E1=DAJN(J)	AIRY259
	F2=0.	AIRY260
	E2=0.	AIRY261
	DO 306 I=1,M3D	AIRY262
	J=J-1	AIRY263
	TEMP1=F1	AIRY264
	TEMP2=E1	AIRY265
	F1 = TT*F1-F2+DAJP(J)	AIRY266
	E1= TT*E1-E2+DAJN(J)	AIRY267
	F2=TEMP1	AIRY268
	E2=TEMP2	AIRY269
306	CONTINUE	AIRY270
	DAI=X*X*(T*F1-F2+DAJP(1))+(T*E1-E2+DAJN(1))	AIRY271
	RETURN	AIRY272
C		AIRY273

Figure A3. (Sheet 21 of 25)

350	CONTINUE	AIRY274
	T=10./C-1.	AIRY275
	TT=T+T	AIRY276
	J=N4	AIRY277
	F1=A(J)	AIRY278
	E1=B(J)	AIRY279
	F2=0.	AIRY280
	E2=0.	AIRY281
	DO 310 I=1,M4	AIRY282
	J=J-1	AIRY283
	TEMP1=F1	AIRY284
	TEMP2=E1	AIRY285
	F1=TT*F1-F2+A(J)	AIRY286
	E1=TT*E1-E2+B(J)	AIRY287
	F2=TEMP1	AIRY288
	E2=TEMP2	AIRY289
310	CONTINUE	AIRY290
	TEMP1=T*F1-F2+A(1)	AIRY291
	TEMP2=T*E1-E2+B(1)	AIRY292
	RTRX=SQRT(RX)	AIRY293
	CV=C-FPI12	AIRY294
	CCV=COS(CV)	AIRY295
	SCV=SIN(CV)	AIRY296
	AI=(TEMP1*CCV-TEMP2*SCV)/RTRX	AIRY297
	J=N4D	AIRY298
	F1=DA(J)	AIRY299
	E1=DB(J)	AIRY300
	F2=0.	AIRY301
	E2=0.	AIRY302
	DO 311 I=1,M4D	AIRY303
	J=J-1	AIRY304
	TEMP1=F1	AIRY305
	TEMP2=E1	AIRY306
	F1=TT*F1-F2+DA(J)	AIRY307
	E1=TT*E1-E2+DB(J)	AIRY308
	F2=TEMP1	AIRY309
	E2=TEMP2	AIRY310
311	CONTINUE	AIRY311
	TEMP1=T*F1-F2+DA(1)	AIRY312
	TEMP2=T*E1-E2+DB(1)	AIRY313
	E1=CCV*CONS+.5*SCV	AIRY314
	E2=SCV*CONS-.5*CCV	AIRY315
	DAI=(TEMP1*E1-TEMP2*E2)*RTRX	AIRY316
	RETURN	AIRY317
	END	AIRY318
	FUNCTION GMLN(X)	GLN1
C	-----	GLN2
C	WRITTEN BY D. E. AMOS, SEPTEMBER, 1977.	GLN3
C	REFERENCES	GLN4
C	* SAND-77-1518	GLN5
C	* COMPUTER APPROXIMATIONS BY J.F.HART, ET.AL., SIAM SERIES IN	GLN6
C	APPLIED MATHEMATICS, WILEY, 1968, P.135-136.	GLN7
C	* NBS HANDBOOK OF MATHEMATICAL FUNCTIONS, AMS 55, BY	GLN8
C	M. ABRAMOWITZ AND I.A. STEGUN, DECEMBER. 1955, P.257.	GLN9
C	ABSTRACT	GLN10

Figure A3. (Sheet 22 of 25)

```

C      GAMLN COMPUTES THE NATURAL LOG OF THE GAMMA FUNCTION FOR      GLN11
C      X.GT.0. A RATIONAL CHEBYSHEV APPROXIMATION IS USED ON        GLN12
C      8.LT.X.LT.1000., THE ASYMTOTIC EXPANSION FOR X.GE.1000. AND  GLN13
C      A RATIONAL CHEBYSHEV APPROXIMATION ON 2.LT.X.LT.3. FOR      GLN14
C      0.LT.X.LT.8. AND X NON-INTEGRAL, FORWARD OR BACKWARD      GLN15
C      RECURSION FILLS IN THE INTERVALS 0.LT.X.LT.2 AND          GLN16
C      3.LT.X.LT.8. FOR X=1.,2.,...,100., GAMLN IS SET TO        GLN17
C      NATURAL LOGS OF FACTORIALS.                                GLN18
C                                                                    GLN19
C      DESCRIPTION OF ARGUMENTS                                    GLN20
C      INPUT                                                       GLN21
C      X      - X.GT.0                                             GLN22
C      OUTPUT                                                GLN23
C      GAMLN  - NATURAL LOG OF THE GAMMA FUNCTION AT X          GLN24
C      -----                                                    GLN25
C      DIMENSION GLN(100),P(5),Q(2),PCOE(9),QCDE(4)             GLN26
C      DATA XLIM1,XLIM2,RTWPIL/ 8. , 1000. , 9.189385332047E-01/ GLN27
C      DATA P(1)/7.663451880000E-04/, P(2)/-5.940956105200E-04/, GLN28
C      1 P(3)/7.936431104845E-04/, P(4)/-2.777777756577E-03/,    GLN29
C      2 P(5)/8.333333333332E-02/                                  GLN30
C      DATA Q(1)/-2.77777777778E-03/, Q(2)/8.333333333333E-02/ GLN31
C      DATA PCOE(1)/2.973786644810E-03/,PCOE(2)/9.238194559028E-03/, GLN32
C      1 PCOE(3)/1.093115956710E-01/,PCOE(4)/3.980671310204E-01/, GLN33
C      2 PCOE(5)/2.159943128461E+00/,PCOE(6)/6.338067999387E+00/, GLN34
C      3 PCOE(7)/2.078247253179E+01/,PCOE(8)/3.603677253002E+01/, GLN35
C      4 PCOE(9)/6.200383800713E+01/                              GLN36
C                                                                    GLN37
C      DATA QCDE(1)/1.000000000000E+00/,QCDE(2)/-8.906016659498E+00/, GLN38
C      1 QCDE(3)/9.822521104714E+00/,QCDE(4)/6.200383800713E+01/ GLN39
C                                                                    GLN40
C      DATA GLN(1) /0.0/, GLN(2) /0.0/, GLN(3) /6.931471805599E-01/, GLN41
C      1 GLN(4) /1.791759469228E+00/, GLN(5) /3.178053830348E+00/, GLN42
C      2 GLN(6) /4.787491742782E+00/, GLN(7) /6.579251212010E+00/, GLN43
C      3 GLN(8) /8.525161361065E+00/, GLN(9) /1.060460290274E+01/, GLN44
C      4 GLN(10)/1.280182748008E+01/, GLN(11)/1.510441257308E+01/, GLN45
C      5 GLN(12)/1.750230784587E+01/, GLN(13)/1.998721449566E+01/, GLN46
C      6 GLN(14)/2.255216385312E+01/, GLN(15)/2.519122118274E+01/, GLN47
C      7 GLN(16)/2.789927138384E+01/, GLN(17)/3.067186010608E+01/, GLN48
C      8 GLN(18)/3.350507345014E+01/, GLN(19)/3.639544520803E+01/, GLN49
C      9 GLN(20)/3.933988418720E+01/, GLN(21)/4.233561646075E+01/, GLN50
C      1 GLN(22)/4.538013889848E+01/, GLN(23)/4.847118135184E+01/, GLN51
C      2 GLN(24)/5.160667556776E+01/, GLN(25)/5.478472939811E+01/, GLN52
C      3 GLN(26)/5.800360522298E+01/, GLN(27)/6.126170176100E+01/, GLN53
C      4 GLN(28)/6.455753862701E+01/, GLN(29)/6.788974313718E+01/, GLN54
C      5 GLN(30)/7.125703896717E+01/, GLN(31)/7.465823634883E+01/, GLN55
C      6 GLN(32)/7.809222355332E+01/, GLN(33)/8.155795945612E+01/, GLN56
C      7 GLN(34)/8.505446701758E+01/, GLN(35)/8.858082754220E+01/, GLN57
C      8 GLN(36)/9.213617560369E+01/, GLN(37)/9.571969454214E+01/, GLN58
C      9 GLN(38)/9.933061245479E+01/, GLN(39)/1.029681986145E+02/ GLN59
C      DATA GLN(40)/1.066317602606E+02/, GLN(41)/1.103206397148E+02/, GLN60
C      1 GLN(42)/1.140342117815E+02/, GLN(43)/1.177718813997E+02/, GLN61
C      2 GLN(44)/1.215330815154E+02/, GLN(45)/1.253172711494E+02/, GLN62
C      3 GLN(46)/1.291239336391E+02/, GLN(47)/1.329525750356E+02/, GLN63
C      4 GLN(48)/1.368027226373E+02/, GLN(49)/1.406739236482E+02/, GLN64
C      5 GLN(50)/1.445657439463E+02/, GLN(51)/1.484777669518E+02/, GLN65

```

Figure A3. (Sheet 23 of 25)

	6	GLN(52)/1.524095925845E+02/,	GLN(53)/1.563608363031E+02/,	GLN66
	7	GLN(54)/1.603311282166E+02/,	GLN(55)/1.643201122632E+02/,	GLN67
	8	GLN(56)/1.683274454484E+02/,	GLN(57)/1.723527971392E+02/,	GLN68
	9	GLN(58)/1.763958484070E+02/,	GLN(59)/1.804562914175E+02/,	GLN69
	1	GLN(60)/1.845338288614E+02/		GLN70
	DATA	GLN(61)/1.886291734237E+02/,	GLN(62)/1.927390472878E+02/,	GLN71
	1	GLN(63)/1.968661816729E+02/.	GLN(64)/2.010093163993E+02/,	GLN72
	2	GLN(65)/2.051681994826E+02/,	GLN(66)/2.093425867525E+02/,	GLN73
	3	GLN(67)/2.135322414946E+02/,	GLN(68)/2.177369341140E+02/,	GLN74
	4	GLN(69)/2.219564418191E+02/,	GLN(70)/2.261905483237E+02/,	GLN75
	5	GLN(71)/2.304390435658E+02/,	GLN(72)/2.347017234428E+02/,	GLN76
	6	GLN(73)/2.389783895618E+02/,	GLN(74)/2.432688490030E+02/,	GLN77
	7	GLN(75)/2.475729140962E+02/,	GLN(76)/2.518904022097E+02/,	GLN78
	8	GLN(77)/2.562211355500E+02/,	GLN(78)/2.605649409719E+02/,	GLN79
	9	GLN(79)/2.649216497986E+02/,	GLN(80)/2.692910976510E+02/,	GLN80
	1	GLN(81)/2.736731242857E+02/,	GLN(82)/2.780675734404E+02/,	GLN81
	2	GLN(83)/2.824742926876E+02/,	GLN(84)/2.868931332954E+02/,	GLN82
	3	GLN(85)/2.913239500943E+02/,	GLN(86)/2.957666013508E+02/,	GLN83
	4	GLN(87)/3.002209486470E+02/,	GLN(88)/3.046868567657E+02/,	GLN84
	5	GLN(89)/3.091641935802E+02/,	GLN(90)/3.136528299499E+02/,	GLN85
	6	GLN(91)/3.181526396202E+02/,	GLN(92)/3.226634991267E+02/,	GLN86
	7	GLN(93)/3.271852877038E+02/,	GLN(94)/3.317178871969E+02/,	GLN87
	8	GLN(95)/3.362611819792E+02/,	GLN(96)/3.408150588708E+02/,	GLN88
	9	GLN(97)/3.453794070623E+02/,	GLN(98)/3.499541180408E+02/	GLN89
	DATA	GLN(99)/3.545390855194E+02/,	GLN(100)/3.591342053696E+02/	GLN90
C		-----		GLN91
	5	NDX=X		GLN92
		T=X-FLOAT(NDX)		GLN93
		IF(T.EQ.0.0) GO TO 51		GLN94
		DX=XLIM1-X		GLN95
		IF(DX.LT.0.0) GO TO 40		GLN96
C				GLN97
C		RATIONAL CHEBYSHEV APPROXIMATION ON 2.LT.X.LT.3 FOR GAMMA(X)		GLN98
C				GLN99
		NXM=NDX-2		GLN100
		PX=PCOE(1)		GLN101
		DO 10 I=2,9		GLN102
	10	PX=T*PX+PCOE(I)		GLN103
		QX=QCOE(1)		GLN104
		DO 15 I=2,4		GLN105
	15	QX=T*QX+QCOE(I)		GLN106
		DGAM=PX/QX		GLN107
		IF(NXM.GT.0) GO TO 22		GLN108
		IF(NXM.EQ.0) GO TO 25		GLN109
C				GLN110
C		BACKWARD RECURSION FOR 0.LT.X.LT.2		GLN111
C				GLN112
		DGAM=DGAM/(1.+T)		GLN113
		IF(NXM.EQ.-1) GO TO 25		GLN114
		DGAM=DGAM/T		GLN115
		GAMLN=ALOG(DGAM)		GLN116
		RETURN		GLN117
C				GLN118
C		FORWARD RECURSION FOR 3.LT.X.LT.8		GLN119
C				GLN120

Figure A3. (Sheet 24 of 25)

22	XX=2.+T	GLN121
	DO 24 I=1,NXM	GLN122
	DGAM=DGAM*XX	GLN123
24	XX=XX+1.	GLN124
25	GAMLN=ALOG(DGAM)	GLN125
	RETURN	GLN126
C		GLN127
C	X.GT.XLIM1	GLN128
C		GLN129
40	RX=1./X	GLN130
	RXX=RX*RX	GLN131
	IF((X-XLIM2).LT.0.) GO TO 41	GLN132
	PX=Q(1)*RXX+Q(2)	GLN133
	GAMLN=PX*RX+(X-.5)*ALOG(X)-X+RTWPIL	GLN134
	RETURN	GLN135
C		GLN136
C	X.LT.XLIM2	GLN137
C		GLN138
41	PX=P(1)	GLN139
	SUM=(X-.5)*ALOG(X)-X	GLN140
	DO 42 I=2,5	GLN141
	PX=PX*RXX+P(I)	GLN142
42	CONTINUE	GLN143
	GAMLN=PX*RX+SUM+RTWPIL	GLN144
	RETURN	GLN145
C		GLN146
C	TABLE LOOK UP FOR INTEGER ARGUMENTS LESS THAN OR EQUAL 100.	GLN147
C		GLN148
51	IF(NDX.GT.100) GO TO 40	GLN149
	GAMLN=GLN(NDX)	GLN150
	RETURN	GLN151
	END	GLN152

Figure A3. (Sheet 25 of 25)

APPENDIX B: NOTATION

$a_0$	Incident wave amplitude
$A_0$	$-iga_0/\omega$
$g$	Gravitational acceleration
$h$	Water depth
$i$	$\sqrt{-1}$
$J$	Bessel function of the first kind
$k$	Wave number
$n$	Non-negative integers
$r$	Polar coordinate
$t$	Temporal coordinate
$x$	Horizontal coordinate
$y$	Horizontal coordinate
$Y$	Bessel function of the second kind
$z$	Vertical coordinate
$\alpha$	Incident wave angle
$\eta$	Free surface displacement
$\theta$	Polar coordinate
$\theta_0$	Angle related to wedge angle
$v$	Value related to wedge angle
$\phi$	Velocity potential function
$\phi$	Horizontal component of the velocity potential function
$\phi_0$	Defined in Equation 12
$\phi_i$	Incident wave velocity potential function
$\phi_r$	Reflected wave velocity potential function
$\phi_s$	Scattered wave velocity potential function
$\bar{\phi}$	Finite cosine transform of $\phi$
$\omega$	Wave radian frequency

END

DATED

FILM

8-88

Dtic